Grain size stabilization of Fe and Fe-Ni nanostructures developed by mechanical alloying

A THESIS SUBMITTED IN PARTIAL FULFILMENT
OF THE REQUIREMENTS FOR THE DEGREE OF

Master of Technology

In

Metallurgical and Materials Engineering

By

DEBASIS NAYAK

Under the Guidance of

Prof. S. C. MISHRA

Department of Metallurgical and Materials Engineering

National Institute of Technology

Rourkela 2013

National Institute of Technology
Rourkela

CERTIFICATE

This is to certify that thesis entitled, ***"Grain size stabilization of Fe and Fe-Ni nanostructures developed by mechanical alloying"*** submitted by Mr. Debasis Nayak in partial fulfillment of the requirements for the award of Master of Technology Degree in Metallurgical and Materials Engineering at National Institute of Technology, Rourkela (Deemed University) is an authentic work carried out by him under our supervision and guidance.

To the best of our knowledge, the matter embodied in this thesis has not been submitted to any other university/ institute for award of any Degree or Diploma.

Prof. S.C.Mishra

Date:

Dept. of Metallurgical and Materials Engineering

National Institute of Technology

Rourkela-769008

ACKNOWLEDGEMENT

I avail this opportunity to extend my hearty indebtedness to my guide **Prof. S. C. Mishra, Dept. of Metallurgical and Materials Engineering, NIT, Rourkela** for their invaluable guidance, motivation, untiring efforts and meticulous attention at all stages during my course of work.

I express my sincere thanks to Prof. B. C. Ray, Head of the Department of Metallurgical and Materials Engineering, NIT, Rourkela for providing me the necessary facilities in the department. I am also grateful to Prof. Krishna Datta M. Tech. co-coordinator, for his constant concern and encouragement for execution of this work.

I also express my sincere gratitude to **Dr. A. Mallik**, **Dept. of Metallurgical and Materials Engineering** and **Dr. Suhrit Mula**, **Dept. of Metallurgical and Materials Engineering, IIT Roorkee** for his timely help during the course of work.

I thankful to Sri Rajesh Pattnaik, Sri Hembram & Sri Udayanath Sahu, Metallurgical & Materials Engineering, Technical assistants, for their co-operation in experimental work.

DATE: DEBASIS NAYAK

ROLL NO. 211MM1364

Abstract

The mechanical alloying (MA) technique has been used to prepare nanocrystalline Fe, Fe-5wt. %Ni, 7 wt. % Ni and 10 wt. % Ni alloys from elemental powder mixtures. Fe-5wt. %Ni and Fe-7 wt. % Ni were detected to form complete solid solution after MA for 1500 min. as per the X-ray diffraction (XRD) analysis. Out these two solid solutions, Fe-7 wt. % Ni alloy was chosen to investigate its grain size stabilization by addition of minute amount of yttrium. Fe is also stabilized by yttrium. All the alloys were annealed at different temperatures up to 1200ºC under high purity argon atmosphere. XRD analysis and microhardness measurement were carried out for all the specimens to analyze their stability after annealing. XRD analysis was carried out to measure the lattice parameter variation due to alloying, which is a vital data to detect whether the solid solution has been formed. Crystallite size was calculated by using Scherer formula and the value of the as-milled sample was below 15 nm. Atomic force microscopy would also be carried for selected specimens to investigate the microstructural features. The experiment showed yttrium stabilizes Fe and Fe-Ni grain size at higher temperature in nano range. Annealing decreases lattice strain for annealing temperature below 900°C but it suddenly increases while annealing at higher temperature for ball milled Fe. With the increase in Ni content upto 5 wt.% lattice strain increases for all annealing temperature except at 700°C and 1200°C. This in term increases its hardness and hence other mechanical properties. Stable crystallite size (less than 100 nm) and constant microhardness of the annealed samples can dictate its usefulness for high strength and other functional applications. Hardness of as milled sample of stabilized Fe obtained to be 9.933 GPa and of Fe-7Ni to be 5.99 GPa. Crystallite size increases with increase in temperature. It becomes stable at higher temperature for Fe-Ni.

Keywords: Grain size stabilization; Vickers hardness; Lattice strain; X-ray diffraction; Atomic force microscopy

CONTENTS

List of figures

List of Figures

List of tables

CHAPTER 1

INTRODUCTION

CHAPTER 1 Introduction

Iron which normally exhibits BCC structure at room temperature may form FCC structure by alloying with different materials has a wide range of applications like structural applications, automobile, making of magnets, other house hold applications etc. Due to its high strength, low cost and availability it is very popular among engineers. So the properties of iron need to be enhanced. This can be improved by making nano structured iron and by solid solution of Iron and other materials like Nickel, Chromium etc. The grain growth while annealing at high temperature can be stabilized by zirconium, yttrium, tantalum etc. [1-3] K.A. Darling et al. found that zirconium is a strong stabilizer and tantalum is a moderate stabilizer of grain of nano crystalline Iron [3].

In this present study nanocrystalline “Fe” and solid solution of “Fe-Ni” are prepared by mechanical alloying (MA). Fe-5wt. %Ni and Fe-7 wt. % Ni were detected to form complete solid solution after MA for 1500 min. as per the X-ray diffraction (XRD) analysis. Out these two solid solutions, Fe-7 wt. % Ni alloy was chosen to investigate its grain size stabilization by addition of minute amount of yttrium.

In the Fe-based powder, with increasing milling time the grain size of the MA powder decreases; however, the decrease in particle size is not linear with milling time. Milling time of 144 h. and more leads to serious cold-welding. The relative density of the as-sintered alloys is influenced by the particle size of the powders before sintering. The coarse particles lead to a low density in the sintered alloys. In the elongated particles the micro hardness is higher than that in the equiaxed grains, the main causes are higher density of the precipitated phase and the larger residual strain [4]. Mechanical milling increases hardness up to 9.5 GPa by the mechanism of grain refinement strengthening of iron–nickel powder. Annealing reduces hardness and induces grain growth. For Fe–8Ni and Fe–10Ni alloys annealed in the two-phase region shows retained austenite, which has a beneficial influence on the cryogenic toughness of ferritic steels. The more the as-milled grain size and defective structure, the more is the possibility of retained austenite. The Vickers hardness of nanocrystalline grains shows less interaction towards Hall–Petch equation rather than coarse-grained powders annealed at high temperatures [5].

In the present study, Fe-Ni nanostructures were developed by mechanical alloying and yttrium is used to stabilize the nanograins of the solid solutions. XRD analysis, annealing under inert atmosphere, AFM and microhardness measurement were used to investigate the stabilization effect of yttrium. Stable crystallite size (less than 100 nm) and constant microhardness of the annealed samples can dictate its usefulness for high strength and other functional applications.

1.1 Aim and Objective

The present study explores the effectiveness of MA for synthesizing the Al-based Al-Si-Ni alloys and the aim of the present study can be enumerated as follows:

- MA of ten Fe-rich compositions, namely (1) Pure Fe, (2) Fe-$Y_{0.25}$ (3) Fe-$Y_{0.5}$, (4) Fe-Ni_5, (5) Fe-Ni_7, (6) Fe-Ni_{10}, (7) Fe-Ni_7-$Y_{0.25}$, (8) Fe-Ni_7-$Y_{0.5}$, (9) Fe-Ni_7-$Y_{0.75}$, (10) Fe-Ni_7-Y_1 (in wt.%) for 1500 min.
- Annealing of the above compositions at 500 °C, 700 °C, 900 °C, and 1200 °C.
- XRD analysis of all the above as-milled and annealed samples.
- Characterize the crystal size, lattice strain and lattice parameter of the above prepared samples by XRD.
- Study of effect of nickel and yttrium content on crystal size, lattice strain and lattice parameter.
- Evaluation of mechanical properties and analysis of the annealed compacts: This would be done by evaluating mechanical properties, namely, microhardness.
- Study of effect of nickel and yttrium content on micro hardness.
- Study of effect of annealing temperature over crystal size and microhardness.
- Characterization of microstructural features of the selected annealed compacts by XRD, AFM to dictate its usefulness for high strength and other functional applications.

CHAPTER 2

CHAPTER 2 Literature Review

2.1 Preamble

Iron is a most useful metal due to its high strength, high flexural rigidity, low cost and availability. It has a wide range of applications like structural applications, automobile, making of magnets, other house hold applications etc. So the properties of iron need to be enhanced. This can be improved by making nano structured iron and by solid solution of Iron and other materials like Nickel, Chromium etc. The grain growth while annealing at high temperature can be stabilized by zirconium, yttrium, tantalum etc. [1-3] K.A. Darling et al. found that zirconium is a strong stabilizer and tantalum is a moderate stabilizer of grain of nano crystalline Iron [3].

High energy ball milling facilitates to produce nanostructured material, which allows powdered samples with different structures and novel properties to be obtained. Due to their small grain size, these materials are characterized by the rather high number of atoms located in the grain boundary. Also, they are very interesting from the magnetic point of view because the grain size approaches that of a magnetic domain, offering thus the possibility to eliminate the influence of the domain walls. It is well established that the intermetallic compounds prepared by mechanical alloying (MA) have a high structural disorder and are unstable.

Cui et al. [6] have studied structure and mechanical properties of high-nitrogen nickel-free austenitic stainless steels with a relative density of 99% fabricated by powder injection molding, conventional sintering, and solidnitriding [6].

D. Cai et al. studied Fe–Ni–Cr alloy system, optimum mechanical properties can be obtained by solution-treated at 1000℃ followed by conventional aging. When the solution temperature is above 1050℃, the flake-like M3B2 precipitates appear along grain boundary and its formation impairs the strength and ductility.

2.2 Different synthesis techniques of nanostructured materials

There are several techniques used to produce nano structured materials, such as (1) Inert gas condensation, (2) rapid solidification processing, (3) electrodeposition, (4) sputtering, (5) crystallization of amorphous phases, (6) chemical processing and (7) Mechanical attrition (ball milling/ mechanical alloying)[7]. Mechanical alloying (MA) is a technique that is used to produce homogeneous nano powders by blending elemental powder mixtures. It involves repeated welding, fracturing, and rewelding of powder particles in a high-energy ball mill. The non-equilibrium phases synthesized include supersaturated solid solutions, metastable crystalline and quasicrystalline phases, nanostructures, and amorphous alloys. Recent advances in these areas and also on disordering of ordered intermetallics and mechanochemical synthesis of materials have been critically reviewed after discussing the process and process variables involved in MA [8].

2.2.1 Importance of Mechanical milling

Mechanical alloying (MA) is a solid-state powder processing technique involving repeated cold welding, fracturing, and rewelding of powder particles in a high-energy ball mill. Earlier, the method of MA was developed in the 1970's for the production of thoria dispersed nickel (TD Nickel) based superalloys. MA has now the capability of synthesizing a variety of metastable phases starting from elemental powder blends to pre-alloyed powders with ductile-ductile or ductile-brittle or brittle-brittle combinations of materials.

Unlike many of the above methods, mechanical attrition produces its nanostructures not by cluster assembly but by the structural decomposition of coarser-grained structures as the result of severe plastic deformation. This has become a popular method to make nanocrystalline materials because of its simplicity, the relatively inexpensive equipment (on the laboratory scale) needed, and the applicability to essentially all classes of materials. The major advantage often quoted is the possibility for easily scaling up to tonnage quantities of material for various applications. Similarly, the serious problems that are usually cited are, (i) contamination from milling media and/or atmosphere [7]; careful attention can reduce/eliminate this problem, and (ii) the need (for structural applications) to consolidate the powder.

2.2.2 Developments in Mechanical alloying (MA)

MA is a capable process to synthesize nanostructured materials presenting improved properties compared to conventional coarse-grained materials [8].

2.2.3 Process Variables

Mechanical alloying is a complex process and hence involves optimization of a number of variables to achieve the desired product phase and/or microstructure. Some of the important parameters that have an effect on the final constitution of the powder are:

- Type of mill
- Milling container
- Milling speed
- Milling time
- Type, size, and size distribution of the grinding medium
- Ball-to-powder weight ratio
- Extent of filling the vial
- Milling atmosphere
- Process control agent
- Temperature of milling

All these process variables are not completely independent. For example, the optimum milling time depends on the type of mill, size of the grinding medium, temperature of milling, ball-to-powder ratio, etc.

Type of mill

There are a number of different types of mills for conducting MA. Depending on the requirements, type of product to be produced, quantity of the product and facilities available, the mills are different. Most commonly, however, the SPEX shaker mills are used for alloy screening purposes. The Fritsch Pulverisette planetary ball mills or the attritor mills are used to produce large quantities of the milled powder. Specially designed mills are used for specific applications.

Milling container

Hardened steel, tool steel, hardened chromium steel, tempered steel, stainless steel, WC-Co, WC- lined steel and bearing steel are used for the grinding vessels. There shouldn't be any cross contamination from milling media and vials. On the other hand, if the two materials are the same, then the chemistry may be altered unless proper precautions are taken to compensate for the additional amount of the element incorporated into the powder.

Milling speed

The efficiency of milling increases with increase in speed. But it shouldn't exceed critical speed of the mill. Above a critical speed, the balls will be pinned to the inner walls of the vial and do not fall down to exert any impact force. Therefore, the maximum speed should be just below this critical value. Another limitation to the maximum speed is the temperature rise during milling. This may be advantageous in some cases where diffusion is required to promote homogenization and/or alloying in the powders. But, in some cases, this increase in temperature may be a disadvantage because the increased temperature accelerates the transformation process and results in the decomposition of supersaturated solid solutions or other metastable phases formed during milling. For this work 400 rpm milling speed is chosen.

Milling time

The time of milling is the most important parameter. Normally the time is so chosen as to achieve a steady state between the fracturing and cold welding of the powder particles. The times required vary depending on the type of mill used, the intensity of milling, the ball-to-powder ratio, and the temperature of milling. The level of contamination increases with milling time and some undesirable phases form. Therefore, it is desirable that the powder is milled just for the required duration and not any longer. Milling time of 50 h was chosen for this work.

Grinding medium

Hardened steel, tool steel, hardened chromium steel, tempered steel, stainless steel, WC-Co, and bearing steel are the most common types of materials used for the grinding medium. It is always desirable to have the grinding vessel and the grinding medium made of the same material as the powder being milled to avoid cross contamination. Stainless steel was used as grinding medium for present study during mechanical milling. The size of the grinding medium also has an influence on the milling efficiency. It has been reported that a combination of large and small size balls during milling minimizes the amount of cold welding and the amount of powder coated onto the surface of the balls.

Ball-to-powder weight ratio (BPR)

The ratio of the weight of the balls to the powder (BPR), sometimes referred to as charge ratio (CR), is an important variable in the milling process. The minimum BPR ranges

from as low as 1:1 to as high as 220:1. In general ratio of 10:1 is most commonly used while milling the powder in a small capacity mill such as a SPEX mill. But, when milling is conducted in a large capacity mill, like an attritor, a higher BPR of up to 50:1 or even 100:1 is used. The ball to powder weight ratio of 10:1 was taken for present study.

Extent of filling the vial

Since alloying among the powder particles occurs due to the impact forces exerted on them, it is necessary that there is enough space for the balls and the powder particles to move around freely in the milling container. Therefore, the extent of filling the vial with the powder and the balls is important. Thus, care has to be taken not to overfill the vial; generally about 50% of the vial space is left empty.

Milling atmosphere

Different atmospheres have been used during milling for specific purposes. Nitrogen or ammonia atmospheres have been used to produce nitrides. Hydrogen atmosphere was used to produce hydrides. The presence of air in the vial has been shown to produce oxides and nitrides in the powder, especially if the powders are reactive in nature. Thus, care has to be taken to use an inert atmosphere during milling.

Process control agents

A process control agent (PCA) is added to the powder mixture during milling to reduce the effect of cold welding. The nature and quantity of the PCA used and the type of powder milled would determine the final size, shape, and purity of the powder particles. Use of a larger quantity of the PCA normally reduces the particle size by 2-3 orders of magnitude. The amount of the PCA is dependent upon the (a) cold welding characteristics of the powder particles, (b) chemical and thermal stability of the PCA, and (c) amount of the powder and grinding medium used. The most important of the PCAs include stearic acid, hexane, Toluene, methanol, and ethanol. Toluene was used as a process control agent for present investigation.

Temperature of milling

There have been conflicting reports on the formation of an amorphous phase as a function of the temperature of milling. Amorphization during MA involves formation of microdiffusion couples of the constituent powders followed by a solid-state amorphization

reaction. Lower milling temperatures are expected to favour amorphization. However, both increased and decreased kinetics have been reported. Milling was carried out in room temperature for present study.

2.2.4 Mechanism of alloying

During milling when two hard balls collide, a very small amount of powder is entrapped in between them. Typically, around 1000 particles are trapped during each collision (Fig. 2.1). The impact force deforms the powder particles plastically leading to work hardening and fracture. The new surfaces created enable the particles to weld together and this leads to an increase in particle size in case of ductile-ductile or ductile-brittle combination of materials.

At this stage, the composite particles have a characteristic layered structure (Fig. 2.3) consisting of various combinations of the starting constituents. With continued deformation, the particles get work hardened and fractured/fragmented of fragile flakes. At this stage, the tendency to fracture dominates over cold welding. Due to the continued impact of grinding balls, the structure of the particles gets steadily refined, but the particle size continues to be the same after certain duration of milling. Steady-state equilibrium is reached when a balance is achieved between the rate of cold welding and the rate of fracturing. At this stage each particle contains substantially all of the starting ingredients in the same proportion of initial composition.

During MA, a variety of crystal defects such as dislocations, vacancies, stacking faults, and increased number of grain boundaries are introduced. The defects such as dislocations, vacancies, stacking faults etc., which are introduced during MA, enhance the diffusivity of solute elements into the matrix. The diffusion distance is also reduced due to refinement of the microstructure. Moreover, the slight rise in temperature of the material during milling also aids the diffusion. Consequently, true alloying takes place amongst the constituent elements [9].

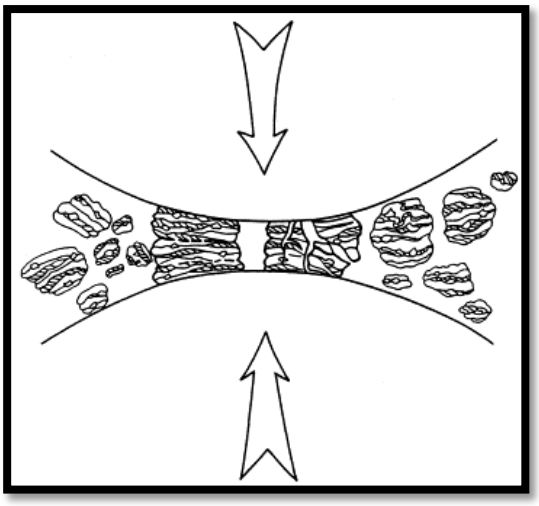

Figure 2.1: Ball-powder-Ball collision of powder mixture during MA

In planetary ball mill the centrifugal force produced by the vials rotating around their own axes and that produced by the rotating support disk both act on the vial contents, consisting of material to be ground and the grinding balls. Since the vials and the supporting disk rotate in opposite directions, the centrifugal forces alternately act in like and opposite directions. This causes the grinding balls to run down the inside wall of the vial- the friction effect, followed by the material being ground and grinding balls lifting off and traveling freely through the inner chamber of the vial and colliding against the opposing inside wall - the impact effect (Fig. 2.2).

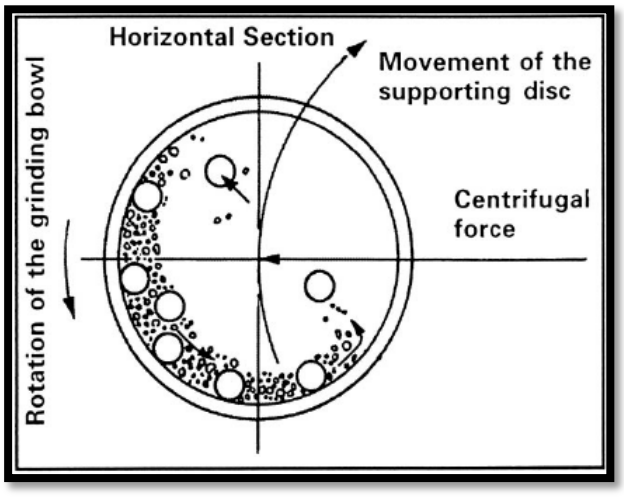

Figure 2.2: Schematic diagram depicting the ball motion inside the ball mill

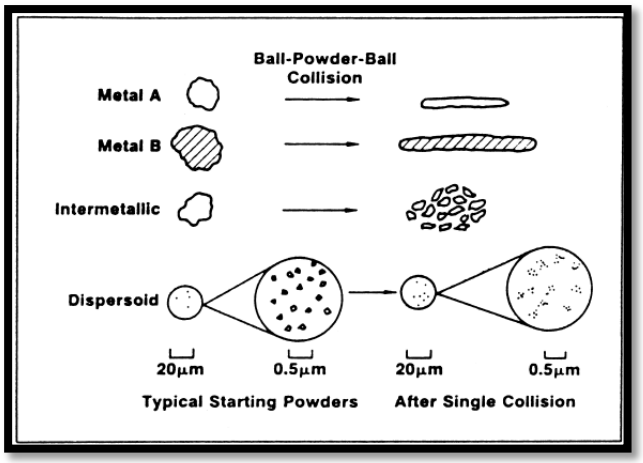

Figure 2.3: Layered structured formed during mechanical alloying.

2.2.5 Advantages of Mechanical Milling (MM)

MM is a simple and an economically feasible process with important technical advantages.

- Usually, we make alloys by melting together the components, whereas, Mechanical alloying involves the synthesis of materials in solid state by high-energy ball milling.
- Bulk material with dimension larger than rapid solidification process (RSP) can be produced by MM.
- Synthesis of novel alloys, e.g., alloying of normally immiscible elements, which is not possible by any other technique like RSP. This is because MM is a completely solid state processing technique and therefore limitations imposed by phase diagrams don't apply here.
- Extended solid solubility was achieved by MM in some alloy system. This technique can be used to induce chemical displacement reactions in powder mixtures at room temperature or at much lower temperature than normally required to synthesize pure metals.
- MM can be used for the refinement of the matrix microstructure down to nanometer range. These nanostructures obtained not by clustered assembly but by the structural decomposition of coarser grained structures as the result of severe plastic deformation.
- Amorphous phase formation is one of the most frequently reported phenomena in mechanically alloyed powder mixtures.

2.3 Mechanical Alloying to prepare Iron based Nanocrystalline

Mechanical deformation under shear conditions and high strain rates ($\sim 10^1$-10^4) leads to the formation of nanostructures within power particles, thin foils or at the surface of metals and alloys exposed to friction induced wear conditions. Solid state (mechanical) alloying beyond the thermodynamic limit can lead to the formation of amorphous metallic materials as observed for a broad range of alloys. During mechanical alloying metals with FCC structure are inherently more ductile and often exhibit a stronger tendency to adhere to the container walls and to sinter into larger particles often several millimetres in diameter. More milling time leads to more strain which implies peak broadening in the x-ray diffraction patterns. The major obstacles for the use of intermetallic compounds as structural materials are their low ductility and toughness at ambient temperature and, in some cases, insufficient strength and creep resistance at high temperatures. While macro alloying or micro alloying has been successful in increasing ductility in specific intermetallic [10].

Previously MA was generally conceived for the production of dispersion strengthened super alloys, is nowadays used for synthesizing a wide range of materials including intermetallics. MA is a solid state, dry milling process that leads, through micro sandwich morphology, to the ultimate mixing of elemental powders and eventually to alloy formation [11].

F. Tehrani et al. studied on the effect of particle size of iron powder on α to γ transformation in the nanostructured high nitrogen Fe–18Cr–10Mn–4Mo stainless steel with two different particle sizes and found that Variations of grain size and internal lattice strain versus milling time, for both iron particle sizes, showed that the critical ferrite grain size for austenite nucleation is less than 10 nm [12]. While synthesizing alloy of Fe–Al–Ni by mechanical alloying F. Hadef et al. found that BCC structured alloy of two different phases with same crystal size but different lattice parameters, proportions and microstrains were developed named as α_1 -Fe(Al, Ni)and α_2 -Fe(Al, Ni). The later one disappears after 4 h and a chemically homogenised structure of α1 -Fe (Al, Ni) lefts behind [13]. By mechanical alloying the solubilities in the Fe–Cu system can be largely extended. It holds good mostly for the single fcc-structure [14].

In the Fe-based powder, with increasing milling time the grain size of the MA powder decreases; however, the decrease in particle size is not linear with milling time. Milling time

of 144 h. and more leads to serious cold-welding. The relative density of the as-sintered alloys is influenced by the particle size of the powders before sintering. The coarse particles lead to a low density in the sintered alloys. In the elongated particles the micro hardness is higher than that in the equiaxed grains, the main causes are higher density of the precipitated phase and the larger residual strain [4].

2.4 Grain growth of Iron based Nanocrystalline prepared by Mechanical alloying

The main objective of mechanical alloying is to produce nanocrystalline material. It also helps in extending solid solution limit in some alloy systems so that properties of the alloy can be increased [7]. Hence it is very important to study the grain growth behaviour of solid solutions prepared by mechanical alloying as, while going through different physical or thermal processing routes the grain growth occurs. The grain growth mechanism of nanocrystalline materials is different than polycrystalline materials [15]. This can be analysed by considering the grain size of a poly crystalline material is very small.

The more is the grain boundary the more is the energy associated with it. So to achieve a stable state, the system leads to reduce the grain boundary by increasing the grain size. The rate of the grain growth shows linear relation with the size of the grain and is inversely proportional [16, 17].

$$dD/dt = k/D \quad (1)$$

Where D is the mean grain diameter after an annealing time t and k is the temperature (T) dependent rate constant.

The integration of the above equation leads to give the grain size D, at t = 0 yields, under ideal conditions.

$$D^2 - D_0^2 = kt. \quad (2)$$

Mostly for high purity metals at high homologous temperatures the grain growth takes place in a parabolic manner. For practical purposes, the most widely used empirical time constant $n \leq 0.5$. By the below equation grain growth under isothermal condition can be described [18].

$$D^{1/n} - D_0^{1/n} = k't \text{ or } D = (k't + D_0^{1/n})^n \quad (3)$$

Pinning forces can affect grain growth in a way that the grain boundary migration may stop before the curvature is completely eliminated. The rate of growth is then proportional to the difference between the curvature of the actual grain size at the given annealing time (l/D) and the curvature of the grain size that corresponds to the limiting curvature where the growth stops (l/D_m):

$$dD/dt = k(l/D - l/D_m) \quad (4)$$

The final form from this analysis is [8]:

$$(D_0 - D)/D_m + In\,[(D_m - Do)/(Dm - D)] = kt \quad (5)$$

Where D_m, is the maximum grain size that results due to the pinning force; k is here given in the units [s^{-1}], but can be expressed in the units [nm^2/s] as $K = kD_m$. The rate constant k (or k') can be expressed in an Arrhenius-type equation:

$$k = k_0 \exp\{ - Q/RT\} \quad (6)$$

Where Q is the activation energy for isothermal grain growth and R is the molar gas constant.

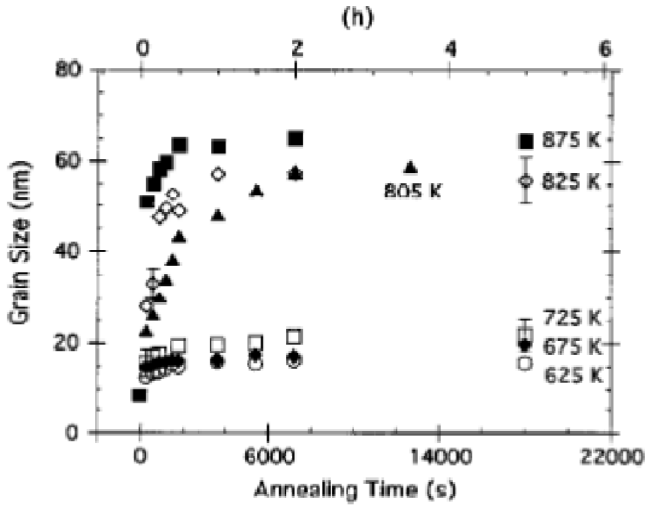

Figure 2.4: Grain size as measured by XRD as a function of annealing time for nanocrystalline Fe annealed at various temperatures between 625 and 875 K [6].

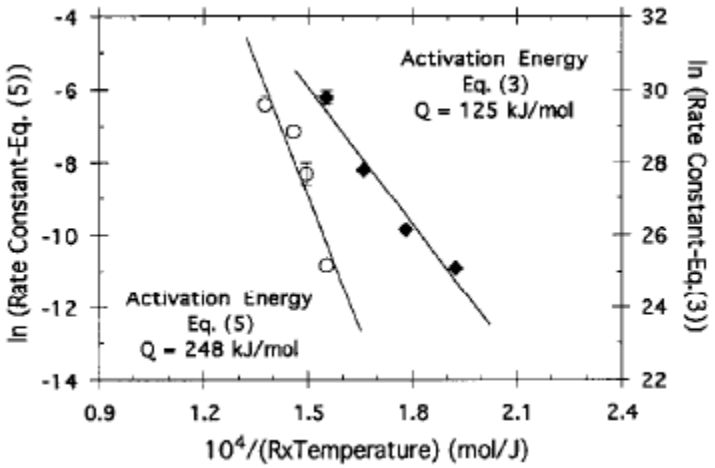

Figure 2.5: Arrhenius plot of grain growth data of nc Fe analysed according to equations (3) and (5). The slope of the linear fit in the plot is used to deduce the activation energy [15].

From the above figure activation energy Q is 125 kJ/mol without considering the pinning force for for an exponent n = 0.083 and Q = 248 kJ/mol considering pinning force. From DSC the obtained value of Q is 224 ± 25 kJ/mol [15].

2.5 Grain growth stabilization

Mechanical properties like hardness, coercitivity, diffusion processes are greatly varied due to microstructure. Grain growth behaviour of different metals and alloys depends upon a number of important variables, which can be defined in terms of mathematical expressions. Titanium, vanadium, zirconium, niobium or aluminium in steels can be used as grain growth stabilizer. This improves quality of structural steel for variety of application. Many researchers have developed both static and dynamic models to minimize grain growth by second phase particles [19, 20].

The variation in the particle radius (r) and volume fraction of precipitates is a function of time and temperature can be represented by Kinetic models. Independent work of Lifshitz and Slyovoz [21] and Wagner [22] reveals how particles coarsen and found that, The kinetics are normally controlled by volume diffusion through the matrix provided the grain boundaries should have a negligible influence on the process. Time dependence of the mean particle radius (r) at steady state given by them is

$$r^3 - r_0^3 = \frac{8\gamma D_m C_m (V_m')^2}{9RT} t \qquad (7)$$

Equation (7) can be applied to continuous heating and cooling. In a more general form this is represented by Lon et al [23].

$$r^3 - r_0^3 = \frac{C_1 t}{T} exp\left(-\frac{Q_s}{RT}\right) \quad (8)$$

Where r_0 is the initial particle radius, V_m' molar volume of precipitate per mole of diffusate (m3/mol), t is time (s), r particle radius (m, μm or nm), D_m is element diffusivity ($\mu m^2/s$, mm^2/s or m^2/s), C_m is concentration of solute in matrix (mol/m 3 or wt. %), R is universal gas constant (8.314 J/K mol), T is temperature (°C or K). The equation (3) suffers from a number of simplifying assumptions.

With the excess amount of solute on the boundary the effective grain-boundary free energy γ per unit area varies according to the Gibbs interface equation

$$d\gamma = -\Gamma d\mu \quad (9)$$

Where Γ is the solute atom excess (mol/area) on a grain boundary and μ is the chemical potential of the solute (energy/mol) [24]. Therefore if solute segregation Γ= 0, then free energy change will be $d\gamma = 0$.

K.A. Darling et al. found that the addition of Ni as segregate to Fe did very little to stabilize against grain growth while Zr had a more significant effect than Ta. Grain growth behaviour is abnormal. The value of abnormality increases with temperature and decreased with solute type as Ni, Ta and Zr respectively [3].

Another method of stabilization is particle pinning. Presence of second phase particles leads to pinning of grain domain boundaries. This effect sets an upper limit to grain size during grain growth (although not necessarily recrystallization). Once a boundary has intersected with a particle, a certain amount of boundary area is removed from the system. In order for the boundary to move off the particle, the "missing area" must be re-created. This restoration of boundary area requires an energy increase. Through the principle of virtual work, this requires a force.

Zener's assumption was that the boundaries can be assumed to intersect randomly with the particles. The fraction of particles with radius r and volume fraction (f) that intersect unit area of a random oriented section plane is $3f/2\pi r^2$. Drag pressure is the product of maximum force per particle and the number per unit area of boundary.

$$P_{drag} = \pi\gamma r * 3f/2\pi r^2 = 3f\gamma/2r \quad (10)$$

The effect of the presence of fine particles is to slow down, and eventually stop grain growth [25].

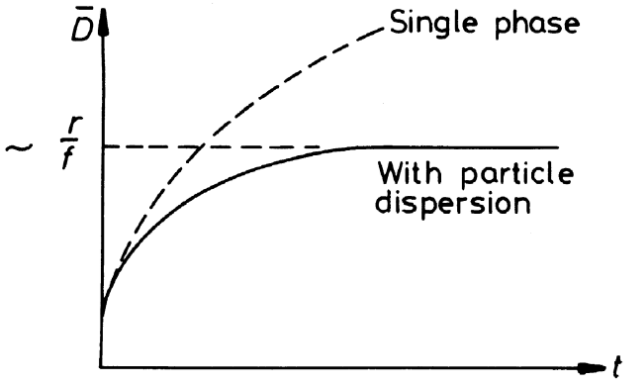

Figure 2.6: Effect of second phase particles on grain growth

The above equation (6) given by Zener based on the assumption that pinning force occurs due to single second phase particle and shape of the particle is spherical so interface between a particle and matrix is incoherent [26], While shape of the particle may be spherical, needle like, plate shaped or cuboidal [26]. N. Moelans et al. found that in pinning columnar grain boundaries nonspherical particles shows better result when the larger side of the columnar grain boundaries are oriented perpendicular to the plane of the film [27]. According to A. Harun et al. pinning geometry of a catenoid of revolution first calculated by Hellman and Hillert, is the minimum energy configuration [28]. K chang et al. found that ellipsoidal particles of eccentricity more than 0.35 are more effective in pinning than cuboidal particle and for eccentricity less than 0.35 cuboidal particles shows better result in pinning [26].

Grain growth can be minimised by rapid solidification of liquid melt. Zheng Chen et al. used this technique to study the grain growth in the undercooled Fe–4 at.% Cu in a controlled way. They proposed a model by which alloy of iron and cupper can be produced in nano scale. The model of grain growth is a combination of kinetic-controlled process, a transition from kinetic mechanism to thermodynamic-mechanism and purely thermodynamic-controlled process [29]. In the above process the effective grain boundary energy is reduced. The driving force can be eliminated by thermodynamic approach, which requires a negative free energy change for segregation of solute atoms from solid solution to grain boundaries [30].

Molinari et al. studied the Role of lattice strain on thermal stability of a nanocrystalline Fe-Mo alloy. They found that crystallite size and average dislocation density is a function of temperature and silica nanoparticles in Fe-Mo alloy decrease the domain size and simultaneously increase the grain-boundary strain in the as-milled powder. Grain-boundary strain stabilizes the domain size. Whose effect is greater than that of the Zener stresses due to grain boundary nanopores and grain boundary silica particles. With the release in certain amount of Zener strain grain growth starts [31].

J. Svejcar et al. investigated different grain growth inhibitors by Energy Dispersive X-RAY analysis. According to their study in a 3% Si-Fe alloys containing various proportions of silicon, sulphur, manganese and iron or aluminium and the smallest particles always contains silicon as the main component which has size of 20-50 nm [32].

Heather A. Murdoch et al. in terms of alloy thermodynamic parameters established a "nanostructure stability map". They developed a model to Stabilize binary nanocrystalline alloys against grain growth and phase separation. The map is given below

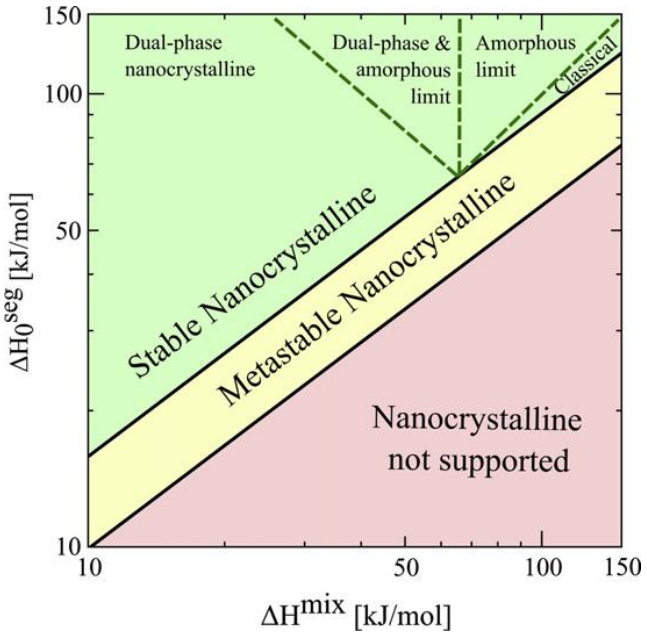

Figure 2.7: Nanostructure stability map, presenting delineated regions of stability (green), metastability (yellow) and no stability (red) in binary alloys as a function of their enthalpies of mixing and segregation. This map is calculated for a fixed dimensionless temperature of 0.35Tcr [33].

From the above figure it is clear that ΔH_0^{seg} should be higher than ΔH^{mix} to get stable nanocrystalline. Different stable nanocrystallines can be obtained which are stable having compositions greater than bulk solubility limit. In the metastable region nanocrystalline are possible with stable grain growth while occurrence of macroscopic phase separation can be observed [33].

2.6 Hardness

Hardness is a measure of how resistant solid matter is to various kinds of permanent shape change when a force is applied. There are three main types of hardness measurements: scratch, indentation, and rebound. Scratch hardness is the measure of how resistant a sample is to fracture or permanent plastic deformation due to friction from a sharp object. Indentation hardness measures the resistance of a sample to material deformation due to a constant compression load from a sharp object; they are primarily used in engineering and metallurgy fields. Rebound hardness, also known as dynamic hardness, measures the height of the "bounce" of a diamond-tipped hammer dropped from a fixed height onto a material. This type of hardness is related to elasticity [34, 35]

Many researchers have worked on nanocrystalline materials and studied their behaviour towards micohardness [36-39] and their result shown gives contradicting picture towards relationship between grain sizes and microhardness, as according to some researchers with decrease in grain size microhardness increases [36-37]while according to others microhardness decreases with decreases in grain size [38, 39]. This can be explained by different metallurgical aspects. According to Hall-Petch equation the relationship between grain sizes and microhardness in coarse-grained materials is

$$Hv = H_0 + kd_1^{-1/2} \qquad (11)$$

Where Hv is the hardness, Ho and k are constants, and d_l is the average grain size. The above equation shows that with decrease in grain size microhardness increases. Nieman et al. [3] reported that nanocrystalline palladium samples (20 nm) show a four-fold increase in hardness compared to coarse- grained (100 μm) palladium and a doubling in hardness for nanocrystalline copper samples (25 nm) over coarse-grained (50 μm) copper [36]. The above equation (1) has limitations because the strength does not increase indefinitely with decreasing grain size as the strength value cannot exceed the theoretical strength, i.e., the

strength of a perfect whisker. Rather fine grain below a certain limit may decrease the strength by softening the material. This can be defined due to Inverse Hall-Petch relation.

Mechanical milling increases hardness up to 9.5 GPa by the mechanism of grain refinement strengthening of iron–nickel powder. Annealing reduces hardness and induces grain growth. For Fe–8Ni and Fe–10Ni alloys annealed in the two-phase region shows retained austenite, which has a beneficial influence on the cryogenic toughness of ferritic steels. The more the as-milled grain size and defective structure, the more is the possibility of retained austenite. The Vickers hardness of nanocrystalline grains shows less interaction towards Hall–Petch equation rather than coarse-grained powders annealed at high temperatures [5].

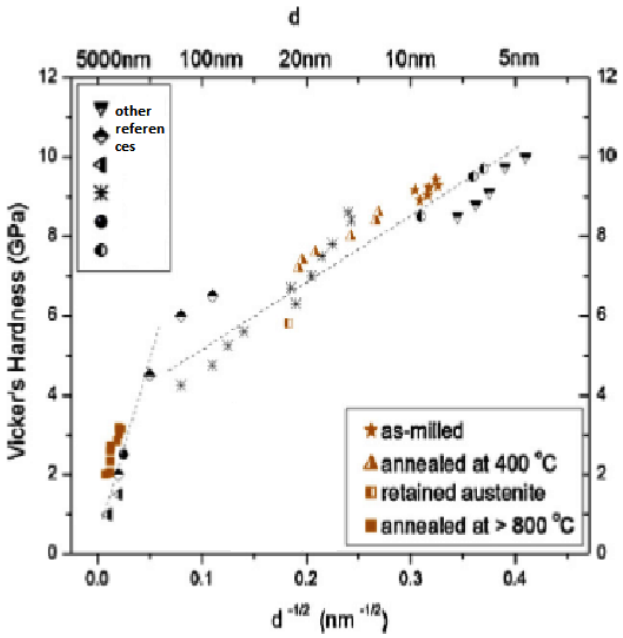

Figure 2.8: Hall–Petch plot of the hardness of as-milled, annealed nanocrystalline and annealed coarse-grained iron and iron–nickel alloys [3].

2.7 Magnetic properties

Iron, some steels, and the naturally occurring mineral lodestone are well-known examples of materials that exhibit magnetic properties.

Microcrystalline ferrites form the basis of materials currently used for magnetic information recording and storage. To increase the recorded information density, it seems reasonable to obtain nanocrystalline ferrites and to prepare magnetic carriers based on them. Grinding of microcrystalline ferrite powders to reach the nanosize of grains is inefficient, as

this gives particles with a broad size distribution, the content of the fraction with the optimal particle size (30 ± 50 nm) being relatively low.

The key method for the preparation of powders of magnetic hexagonal ferrites with a grain size of more than 1 mm includes heating of a mixture of the starting compounds at temperature above 1000℃ (so-called ceramic method). An attempt has been made 79 to use this method for the synthesis of barium ferrite nanoparticles. The initial components (barium carbonate and iron oxide) were ground for 48 h in a ball mill and the resulting powder was mixed for 1 h at a temperature somewhat below 1000℃. This gave rather large particles (200 nm and greater) with a broad size distribution. Similar results have been obtained in the mechano- chemical synthesis of barium ferrite from BaCl2, FeCl3 and alkali with subsequent oxidative annealing [40].

Iron-based alloys are one of the most components of soft magnetic composite materials (SMCs). H. Shokrollahi found that by addition of alloying elements or change in composition a wide range of magnetic alloys with different magnetic and electrical properties can be achieved. These alloys are binary (Fe–X), ternary (Fe–X–Y) or higher component systems. A useful method for production of iron-based alloys with different composition and particle size is mechanical alloying. Mechanical alloying of magnetic Fe-based alloys led to the formation of supersaturated solid solution, multiphase or possibly amorphous structure. The introduction of Si into Fe can result in a decrease of magnetic anisotropy and enhance electrical resistivity in Fe–Si alloys. Fe–Co alloys exhibit high saturation magnetization and high Curie temperature. The addition of Ni to iron-based alloys increases permeability, saturation magnetization and resistivity. The addition of Si into Fe can enhance the electrical resistivity and decrease the anisotropy and also Ni addition can increase saturation magnetization, permeability and resistivity. The addition of Boron can increase the surface energy in Fe-based powders and saturation magnetization in Fe-based alloys [41].

The bulk samples of the iron-nickel alloys are either nonmagnetic or are magnetically soft ferromagnets (for example, permalloys containing >30% of Ni and various doping additives). When the content of nickel is ~30%, their magnetic properties approach the properties of invar (36% of Ni, 64% of Fe, about 0.05% of C). The Fe-Ni nanoparticles have a much lower saturation magnetisation than the corresponding bulk samples over the whole concentration range [42]. An alloy containing 37% of Ni has a low TC and a FCC structure. It consists of nanoparticles (12-80 nm) superparamagnetic over a broad temperature range

[43]. Theoretical calculations predict a complex magnetic structure for these Fe ± Ni particles (clusters) [44].

Yongsheng Liu et al. fabricated soft magnetic alloy with Ni-doping by high-energy milling. They found that the nickel doped decreases the resonance frequency of Fe–Ni alloy, but Ni doping enhances the frequency stability. The corresponding value of initial permeability as a function of Ni doping concentration was given at 10 kHz and the result indicates that the peak value of initial permeability shifts to the region of low Ni concentration for the samples milled for 72 h [45].

R. Hamzaoui et al. used ANN method to optimization of magnetic properties of iron based magnetic materials. They studied the compositions Fe–20 wt. % Ni and Fe–6.5 wt.% Si, alloys, obtained using two high-energy ball milling technologies. Same method was also used by R. Hamzaoui et al. to to predict magnetic properties of mechanically alloyed Fe–10%Ni and Fe–20%Ni nanocrystalline. They found that the higher the speed rotation of the rotation speed of the disc on which the vial holders are fixed (Ω) and the lower speed rotation of the vial holders turn at a rotation Speed(ω), the larger the coercivity Hc, the lower the speed rotation Ω and the higher the speed rotation ω, the lower the coercivity Hc. Experimental milling conditions corresponding to the lowest value of the speed rotation Ω and to the highest value of the speed rotation ω were found to lead to the formation of alloys exhibiting a soft magnetic behaviour for both Fe–10%Ni and Fe–20%Ni alloys [46].

2.8 Corrosion

Nanocrystalline can be produced by processes such as sputtering, electron beam evaporation, pulse laser ablation, gas condensation and sol–gel method. However, the use of these techniques for processing nanocrystalline materials is limited to thin films or small samples, whereas it is necessary to produce/process bulk samples for corrosion or mechanical testing. Electrodeposition and severe plastic deformation have been recognised as the two relatively successful routes for processing nanocrystalline materials [47].

Nickel Provides metallurgical stability, improves thermal stability and weldability, improves resistance to reducing acids and caustics, and increases resistance to stress corrosion cracking particularly in chlorides and caustics. Because of soft magnetic properties, thermal expansion and corrosion resistance iron-nickel alloy have great

commercial interest. Electrodeposition of nanostructured alloys of Iron-Nickel provides great strength, corrosion resistance, increased wear resistance and soft magnetic properties [48].

A. Baron et al. studied the Corrosion of amorphous and nanocrystalline Fe-based alloys and its influence on their magnetic behaviour. They found that Stability of $Fe_{78}Si_9B_{13}$ and $Fe_{73.5}Si_{13.5}B_9Nb_3Cu_1$ magnetic alloys is a function of their chemical composition, struc 0.8 T before corrosion, to Bs = 0.67-0.70 T after corrosion in chlorides. On the basis of the tests we can state that the applicable structures of both alloy are not enough for achieved good corrosion resist in research condition, chlorine solution. Corrosion rate of the amorphous relaxed Fe78Si9B13 alloy amount 0.36 mm/year, and nanocrystaline equivalent corroding rate amount 0.13 mm/year. Corrosion rate of nanocrystalline $Fe_{73.5}Si_{13.5}B_9Nb_3Cu_1$ alloy amount 0.31 mm/year, but the highest corrosion resist were observed for amorphous "as received" ribbon of this alloy (0.12 mm/year). The similarity between the impedance spectrums of both alloys in amorphous state in chlorine solution can be attributed to their very similar structures properties despite their different chemical composition. Heat treatment of amorphous precursor leads to appear significant changes in corrosion behavior. It seems most likely the Si element plays important role in corrosion resistance of nanocrystalline $Fe_{78}Si_9B_{13}$ alloy and it responses for formation passive layer. Nanocrystallization of amorphous $Fe_{73.5}Si_{13.5}B_9Nb_3Cu_1$ alloy favour formation of composite passive layer consists of a porous external film and a homogenous internal one which displayed good protective properties [49].

CHAPTER 3

CHAPTER 3 Experimental

This chapter deals with the details of the experimental procedures carried out in this investigation. The materials were subjected to a series of characterizations, e.g., microstuctural characterization by X-ray diffraction (XRD) and atomic force microscopy (AFM). Mechanical properties like Vickers hardness measurement. The details of each process are described in the following sections.

3.1 Development of Fe-based nanocrystalline material

In the present investigation mechanical milling was carried out for preparation of 10 compositions, namely, (1) Pure Fe, (2) Fe-$Y_{0.25}$ (3) Fe-$Y_{0.5}$, (4) Fe-Ni_5, (5) Fe-Ni_7, (6) Fe-Ni_{10}, (7) Fe-Ni_7-$Y_{0.25}$, (8) Fe-Ni_7-$Y_{0.5}$, (9) Fe-Ni_7-$Y_{0.75}$, (10) Fe-Ni_7-Y_1 (in wt.%). Milling was carried out in the argon atmosphere to maintain inertness. Fe-5wt. %Ni and Fe-7 wt. % Ni were detected to form complete solid solution after MA for 1500 min. as per the X-ray diffraction (XRD) analysis. Out these two solid solutions, Fe-7 wt. % Ni alloy was chosen to investigate its grain size stabilization by addition of minute amount of yttrium.

3.1.1 Mechanical milling

The elemental powders of Fe, Ni, Y (purity >99.0 %) were used to blend the compositions mentioned above. These were subjected to high energy milling in the stainlesssteel grinding media at a mill speed of 1725 r.p.m. by means of a Spex 8000M Ball Mill (Zirconia & Steel mill sets). The ball to powder weight ratio was 10:1. Powder samples were prepared weighing 5.1 gram each. Milling was carried out for 1500 min for all the samples. Pellets were made by a hydraulic compacting machine at 6.5 ton and a dwelling period of 90 second. Poly vinyl chloride (PVC) was used as binder.

Figure 3.1: Spex 8000M Ball Mill, (Zirconia & Steel mill sets)

3.1.2 Annealing of pellets

All the samples were annealed at temperatures of 500°C, 700°C, 900°C and 1200°C. This was done in the argon atmosphere, so as to provide inert atmosphere. Cooling was done in the furnace. Annealing was done in a wide range of temperature and at higher temperatures to study the grain growth behaviour and stability of Fe and Fe-Ni by yttrium. Annealing at higher temperature leads to sintering also. All the annealed samples and powder compacts were studied by XRD to know the crystallite size and lattice strain.

3.2 Microstructural characterization

3.2.1 X-ray Diffraction (XRD)

The phase evolution at different stages of mechanical milling were studied by XRD analysis using the Cu Kα (λ=1.542Å) in a Philips X-pert MPD X-ray diffractometer. XRay diffraction patterns were recorded from 25° to 100° with an accelerating voltage of 30 kV. Data were collected with a counting rate of 3°/min. The average crystallite size of all the samples was determined from the broadening of Cu reflection after stripping of Kα2 component using Scherrer formula. For the overlapping peaks, the fullwidth at half intensity maximum and the true Bragg angle (2θ) were determined by an appropriate deconvolution exercise.

Figure 3.2: Philips X-pert MPD X-ray diffractometer.

The Scherrer equation can be written as:

$$D = \frac{K\lambda}{\beta cos\theta} \quad (12)$$

And lattice strain (LS) is

$$LS = \frac{\beta}{4tan\theta} \quad (13)$$

Where

- D is the mean size of the ordered (crystalline) domains, which may be smaller or equal to the grain size
- K is a dimensionless shape factor, with a value close to unity. The shape factor has a typical value of about 0.9, but varies with the actual shape of the crystallite
- λ is the X-ray wavelength

- β is the line broadening at half the maximum intensity (FWHM), after subtracting the instrumental line broadening, in radians. This quantity is also sometimes denoted as $\Delta(2\theta)$
- θ is the Bragg angle.

3.2.2 Atomic Force Microscopy (AFM)

VEECO di Innova atomic force microscope was utilized to study AFM micrograph of few annealed samples. In the present investigation this instrument is mainly used to find out the average particle size of specimens and to study whether it is best suited with the crystallite size got from XRD.

Figure 3.3: VEECO di Innova atomic force microscope.

3.3 Evaluation of Mechanical Properties

3.3.1 Micro Hardness Measurement

Vickers hardness tester (Leco LV 700) was used to determine Vickers hardness values of all the sintered specimens using 50 gram load for a dwell time of 15 s. The variation in the hardness values obtained for a particular specimen was ±10 Hv.

Figure 3.4: Leco LV 700 Vickers hardness tester

CHAPTER 4

RESULT AND DISCUSSION

CHAPTER 4 Result and Discussion

4.1 Structural Characterization of Milled Samples

The structural characterizations of the mechanically milled powder samples were carried out by XRD.

4.1.1 XRD analysis of Fe and Fe-Y system

XRD is a very good characterisation technique used to determine the crystallite size and lattice strain of different materials.

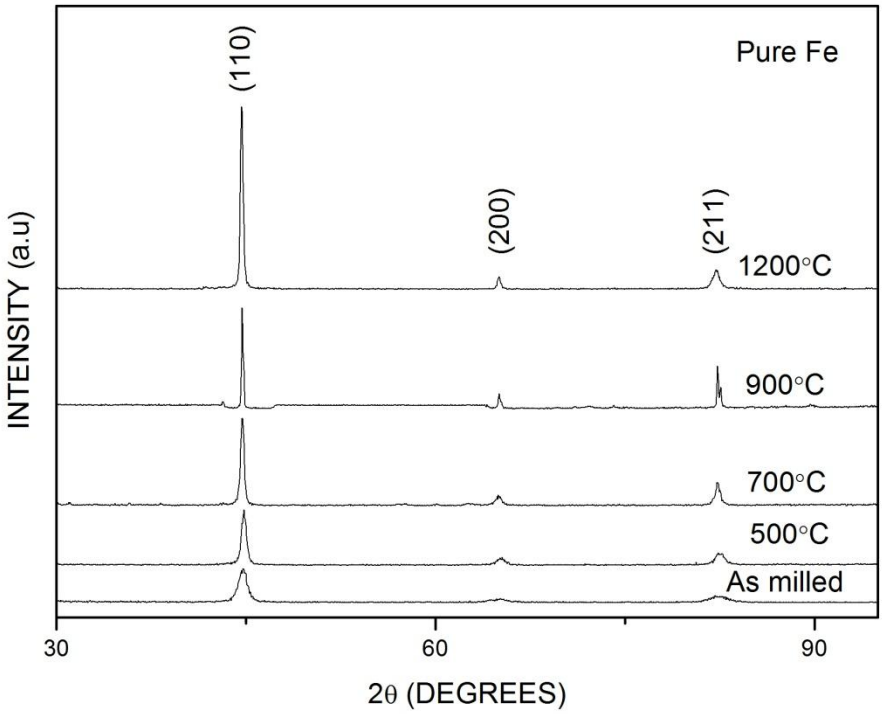

Figure 4.1: XRD pattern of pure Fe at different temperature

The above figure shows XRD pattern of pure Fe annealed at different temperatures. The XRD peaks of the samples are (110), (200) and (211).

In the above figure the more is the lattice strain for wider peaks which will be discussed later. Peak intensity increases with increase in temperature.

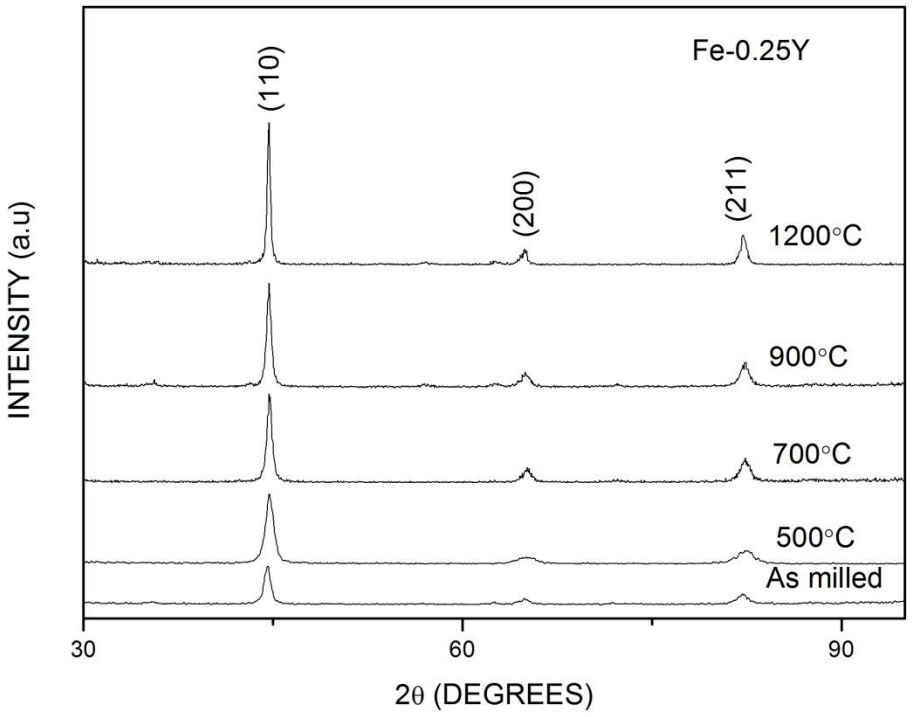

Figure 4.2: XRD pattern of Fe-0.25 wt.% Y at different temperature

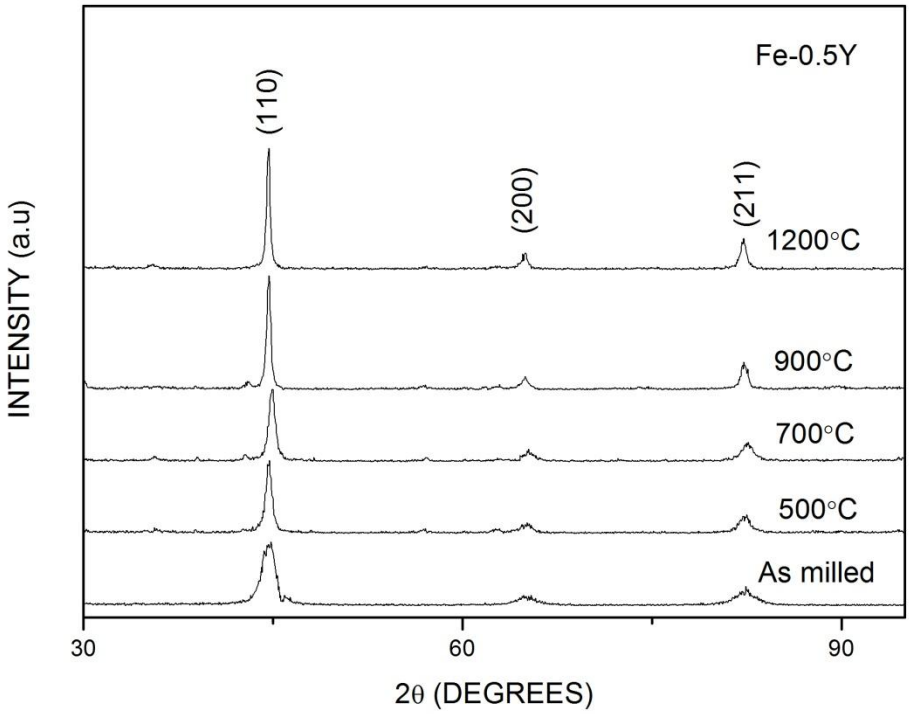

Figure 4.3: XRD pattern of Fe-0.5 wt.% Y at different temperature

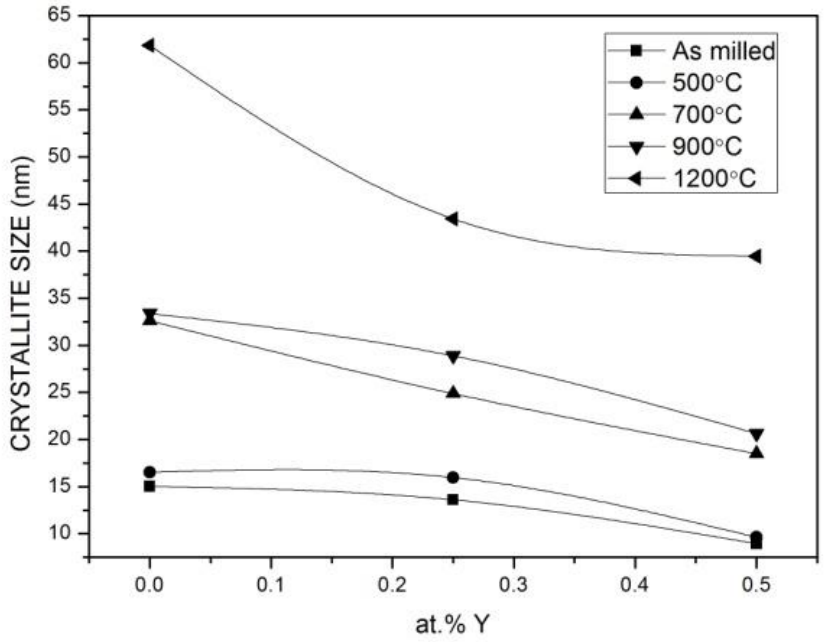

Figure 4.4: Variation of crystallite size at different temperatures with addition of yttrium in Fe

Crystallite size decreases with increase in yttrium content. K.A. Darling et al. [3] found that yttrium is a good stabilizer of grain growth than zirconium, tantalum, chromium and nickel. The above sequence of materials depicts the stabilizing effects in a decreasing manner. The increase in solute concentration decreases the grain boundary energy, hence the formation of grain boundary requires less energy to be formed. This leads to formation of new and fine grains. The tendency of the system to be favourable in lowest possible energy is satisfied by addition of these solutes.

In binary systems, configurations can exist which allow for the local minimization of the system's energy to take place by mechanisms other than grain growth. The absorption of impurity atoms within the excess grain boundary area available in nanocrystalline materials leads to reduce the grain boundary energy. Gibbs interface absorption equation can define this condition. The simplified Gibbs adsorption equation in the dilute limit, the effective grain boundary energy γ, as a function of the segregated solute content is [50–53].

$$\gamma = \gamma_0 + \Gamma_s + [\Delta H_{seg} - T\Delta S_{seg}] \quad (12)$$

Here γ_o is the grain boundary energy of a random solid solution, Γ_s is the specific interfacial solute excess and ΔHseg and ΔSseg are the enthalpy and entropy changes associated with segregation of solutes from the matrix to the grain boundaries respectively, when [ΔHseg −TΔSseg] < 0, solute segregation to the grain boundary is favoured and γ decreases.

From the figure 4.4, it is clear that crystallite size decrease with yttrium content. For pure iron milled for 1500 minutes leads to formation of crystallite size of nanocrystalline material of about 15nm. The addition of yttrium about atomic per cent of 0.5 leads to

formation of grain size of about 8nm.

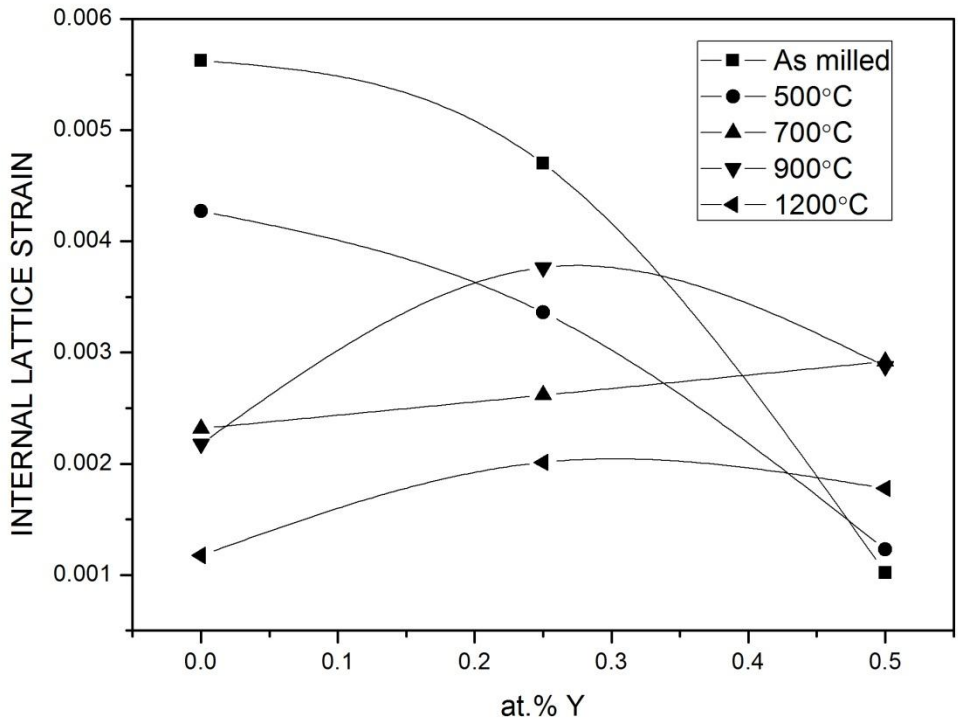

Figure 4.5: Variation of Lattice Strain at different temperatures with addition of yttrium.

The figure 4.5 depicts the variation of internal lattice strain with addition of yttrium. The more is the yttrium content the less is the internal lattice strain for as milled samples and samples annealed at 500℃, But with subsequent increase in temperature it increases first till 0.25 atomic per cent of yttrium and then decreases for 900℃ and 1200℃. but still increases for 700℃. Again internal lattice strain decreases with increase in temperature. Variation to the previous statement can be seen for 0.25 atomic per cent of yttrium, where internal lattice strain is more at 900℃ than 500℃ and for 0.5 atomic per cent of yttrium internal lattice strain is in increasing order is as milled, 500℃, 1200℃, 900℃, 700℃.

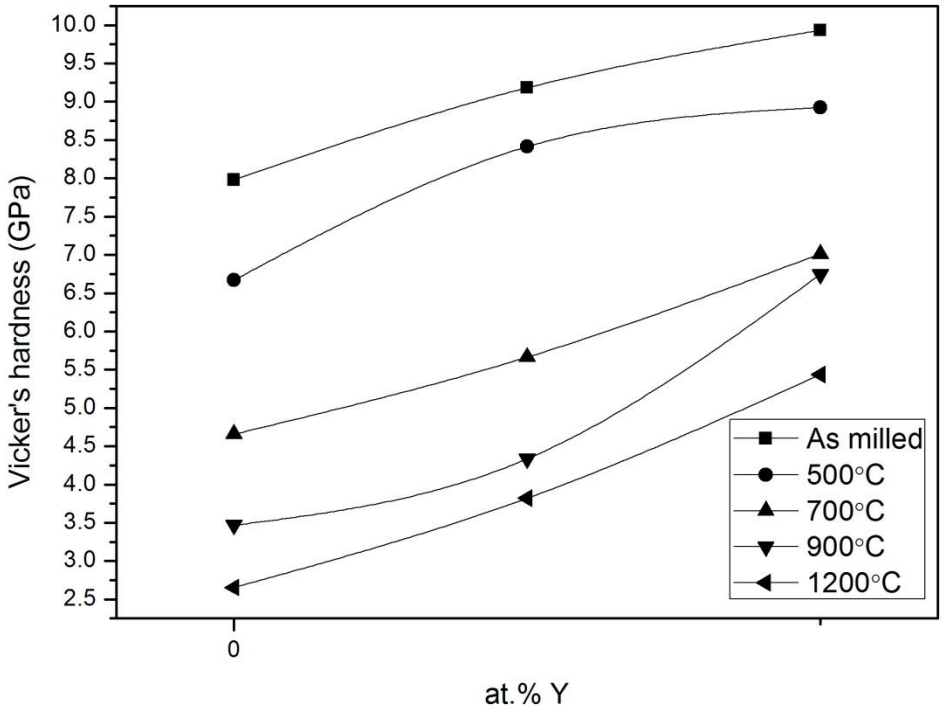

Figure 4.6: Variation of Micro hardness at different temperatures with addition of yttrium.

Addition of yttrium increases hardness from 8 GPa up to 10 GPa for as milled samples. Hardness decreases with increase in temperature, this happens due to increase in crystallite size. Softening occurs due to annealing at higher temperature.

The rate of increase in hardness is almost constant over the composition variation.

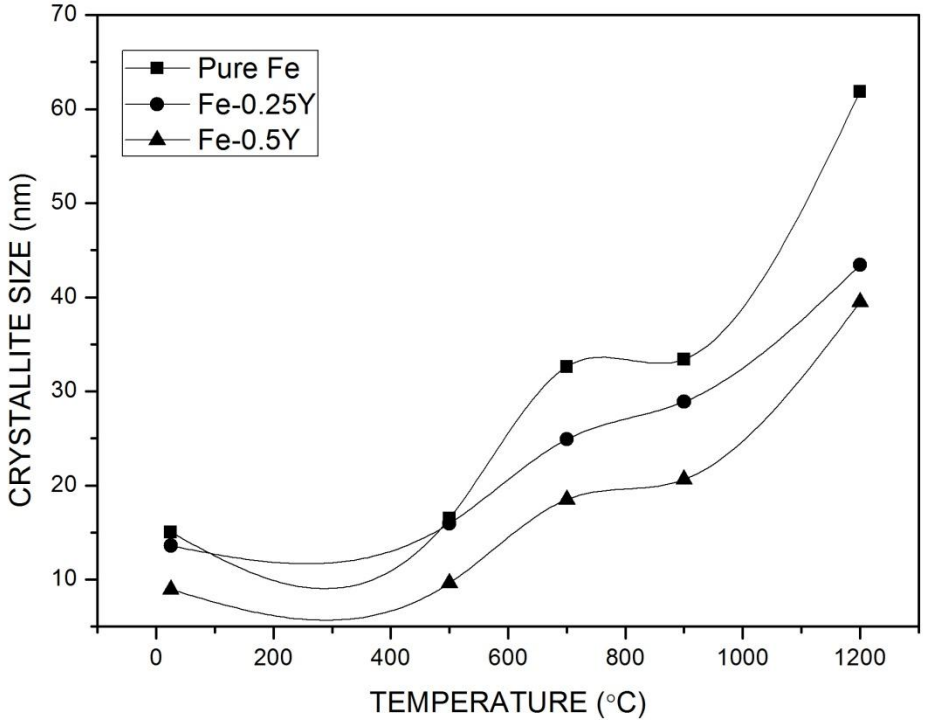

Figure 4.7: variation of crystallite size with different temperature of various compositions

The Figure 4.7 depicts variation of crystallite size with different temperature of various compositions. Crystallite size increases with increase in annealing temperature. The higher the annealing temperature, the rate of increase in crystallite size is more for all compositions. Annealing temperature up to 500℃ the increase in crystallite size is negligible.

This can be explained by both equation 1 and equation 6. The more is the grain boundary the more is the energy associated with it. So to achieve a stable state, the system leads to reduce the grain boundary by increasing the grain size. The rate of the grain growth shows linear relation with the size of the grain and is inversely proportional [16, 17].

$$dD/dt = k/D \quad (1)$$

Where D is the mean grain diameter after an annealing time t and k is the temperature (T) dependent rate constant. And the rate constant k is

$$k = k_0 \exp\{ - Q/RT\} \quad (6)$$

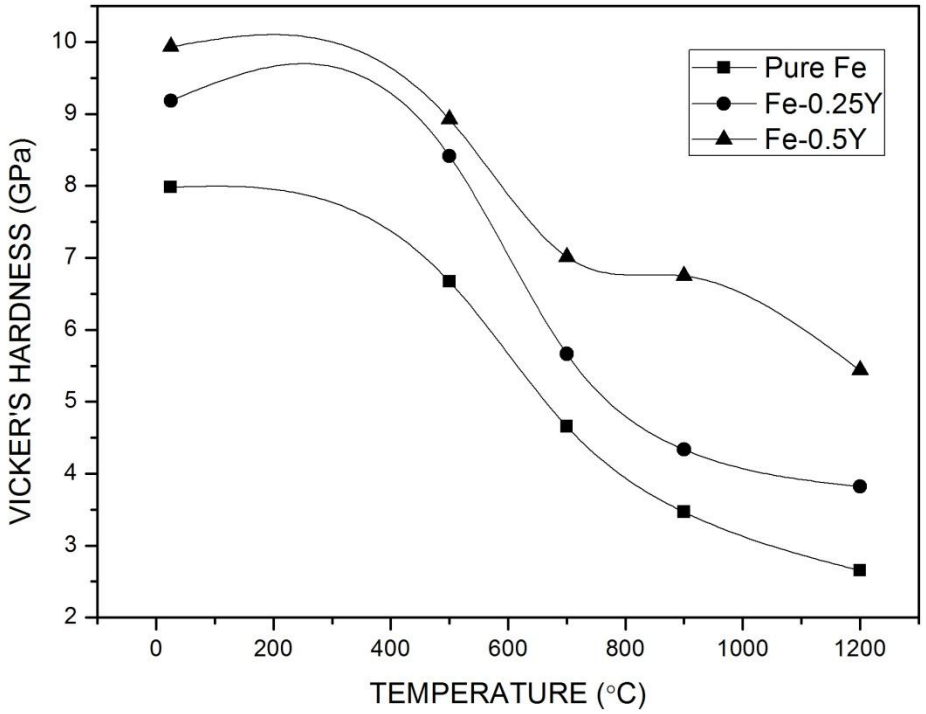

Figure 4.8: variation of Micro hardness with different temperature of various compositions

The Figure 4.8 depicts variation of Micro hardness with different temperature of various compositions. Increase in temperature leads to decrease in micro hardness. This happens due to increase in grain growth and softening of the material.

4.1.2 XRD analysis of Fe-Ni system

Addition of Ni helps in stabilizing grain growth. K.A. Darling et al. found that the addition of Ni as segregate to Fe did very little to stabilize against grain growth while Zr had a more significant effect than Ta. Grain growth behaviour is abnormal. The value of abnormality increases with temperature and decreased with solute type as Ni, Ta and Zr respectively [3].

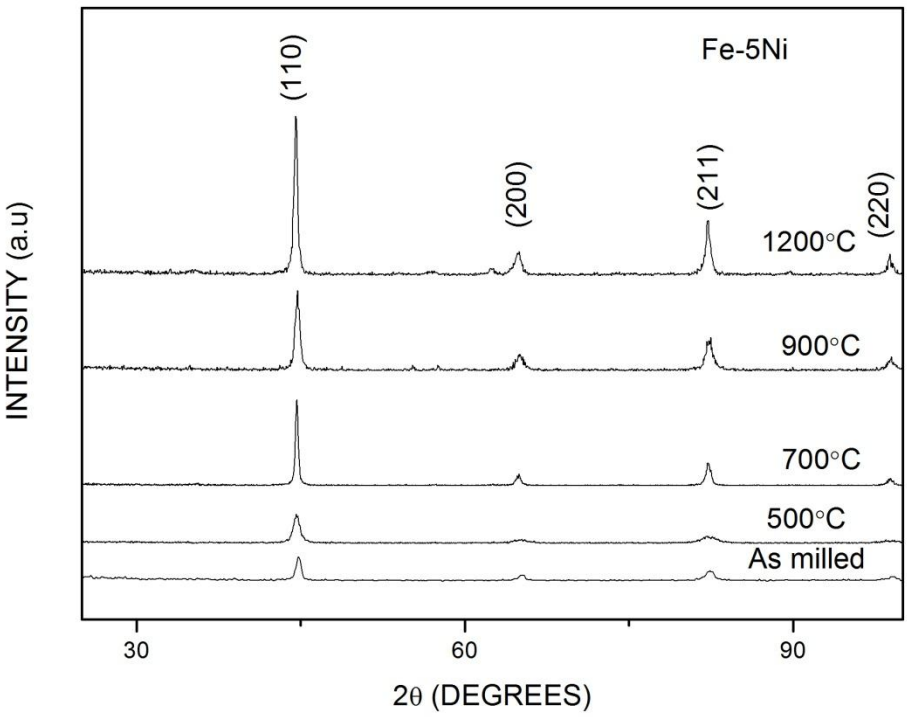

Figure 4.9: XRD pattern of Fe-5 wt. % Ni at different temperature

The above figure shows XRD pattern of pure Fe annealed at different temperatures. The XRD peaks of the samples are (110), (200) and (211).

In the above figure the more is the lattice strain for wider peaks which will be discussed later. Peak intensity increases with increase in temperature.

Figure 4.10 and 4.11 shows XRD pattern of Fe-7 wt. % Ni and Fe-10 wt. % Ni at different temperature respectively.

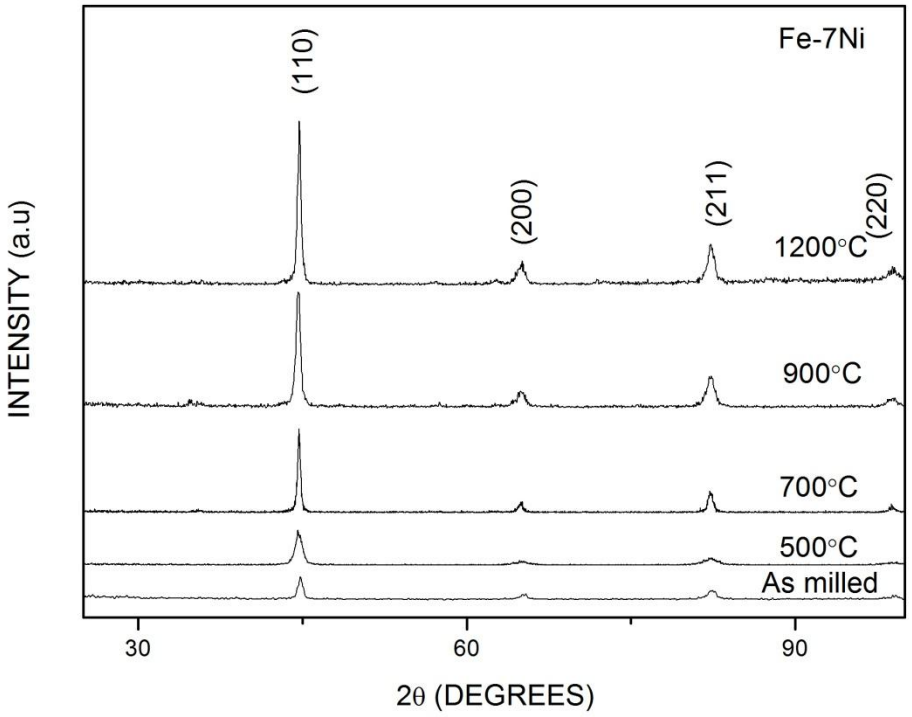

Figure 4.10: XRD pattern of Fe-7 wt.% Ni at different temperature

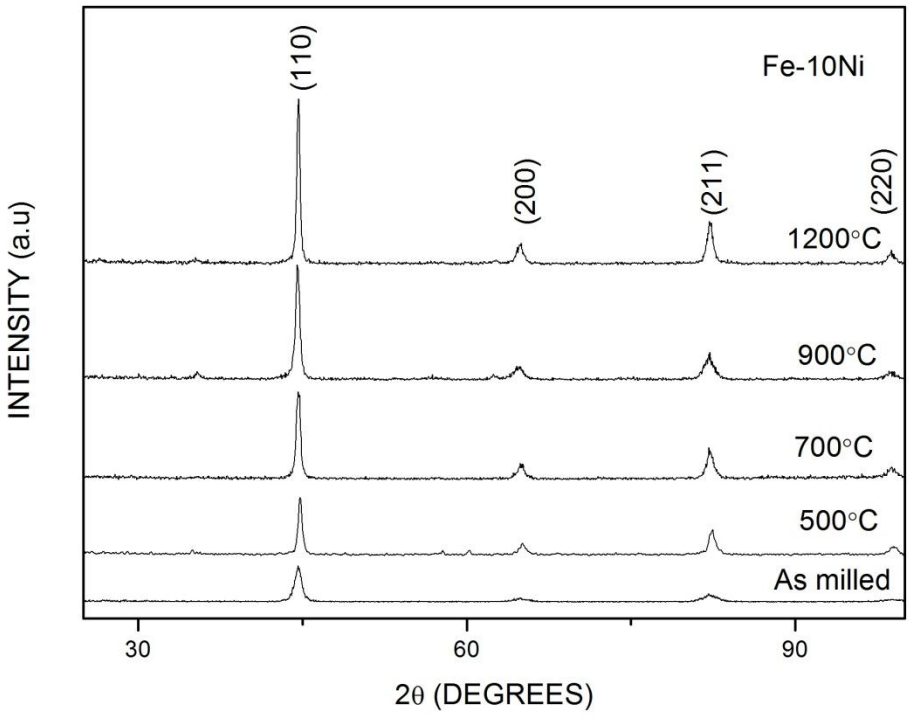

Figure 4.11: XRD pattern of Fe-10 wt.% Ni at different temperature

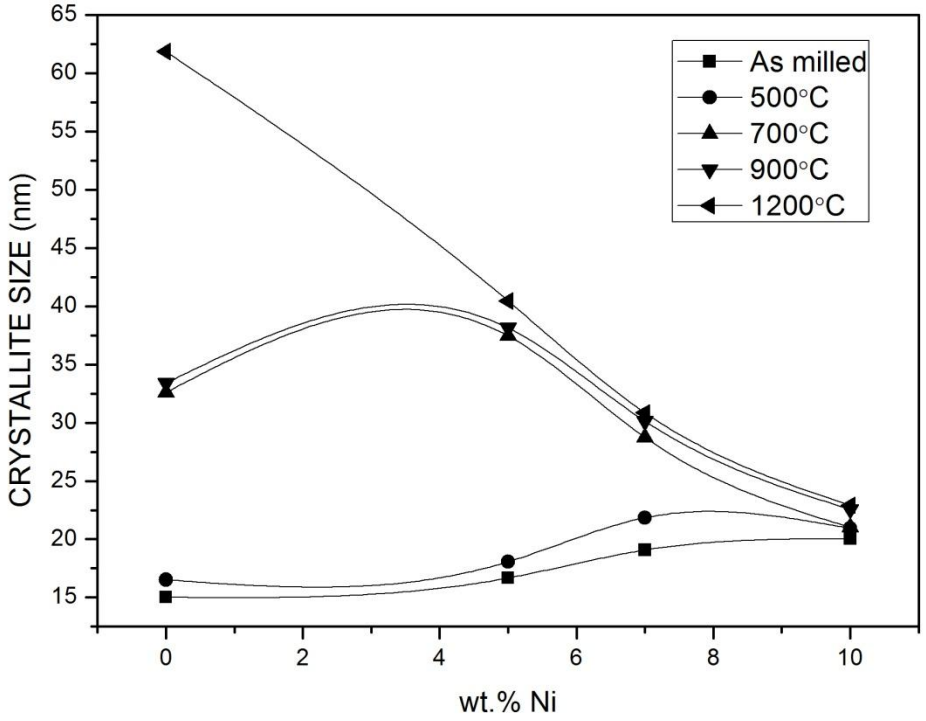

Figure 4.12: Variation of crystallite size at different temperatures with addition of Ni with Fe

The figure 4.12 shows the Variation of crystallite size at different temperatures with addition of Ni with Fe. The crystallite size increases with the increase in Ni content up to 10 wt. % for as milled sample and annealed at 500℃. when annealed at 700℃ and 900℃ the crystallite size increases up to 5 wt. % of nickel. Then the crystallite size decreases with subsequent addition of Ni. When the samples with varying Ni content annealed at 1200℃, it is seen that crystallite size always decreases with increase in Ni wt. %.

The possible reason to explain the increase in crystallite size is, the grain boundary energy increases with the increase in Ni content. So formation of new grain boundary to make fine grains is hindered. Annealing at higher temperature and Ni content provides energy to minimize the grain boundary energy, so crystallite size decreases [3].

On thermal stability of nanocrystalline Fe, Ni has the less influence and was therefore selected as a control because of its low atomic mismatch and low elastic strain enthalpy. Ni

shows complete solid solubility in Fe at high temperatures and therefore exhibits a small enthalpy of mixing term [53, 54].

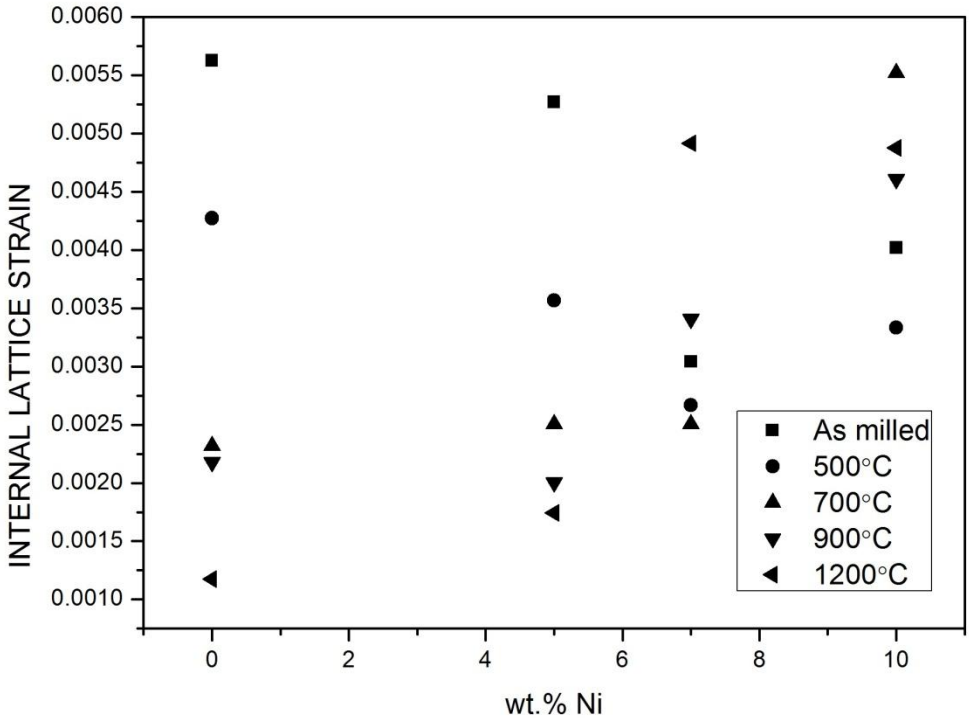

Figure 4.13: Variation of Lattice strain at different temperatures with addition of Ni with Fe

Figure 4.13 shows Variation of Lattice strain at different temperatures with addition of Ni with Fe, for pure iron internal lattice strain decreases with increase in temperature. With increase in Ni content up to 7 wt. % the lattice strain decreases, while further increase in Ni lead to increase in it for as milled sample and annealed at 500℃. The XRD peaks also reveal the same.

It was reported by A. Revesz et al. [53] that dislocations are the primary cause of strain in ball milled iron.

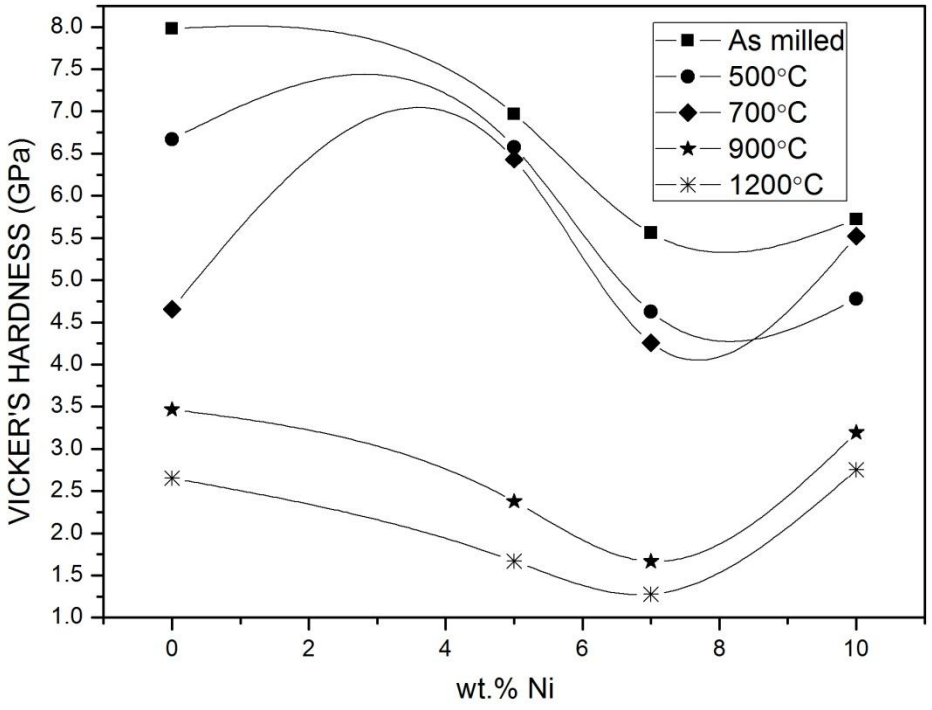

Figure 4.14: Variation of Micro hardness at different temperatures with addition of Ni with Fe

Figure 4.12 shows variation of Micro hardness at different temperatures with addition of Ni with Fe. With increase in Ni content up to 7 wt. % hardness decreases. But further increase in nickel leads to increase in micro hardness. Again increase in temperature decreases micro hardness. Variation to the above pattern can be seen for annealing at 700℃. Here hardness increases with increase in Ni content up to 5 wt. %.

Decrease in micro hardness is due to increase in crystallite size for as milled samples and samples annealed at 500℃, this obeys Hall-petch relation [36-39]. But for higher annealing temperature with decrease in crystallite size also do not helps in increase in hardness. This can be defined due to Inverse Hall-Petch relation. H. Kotan et al. found that Vickers hardness of nanocrystalline grains shows less interaction towards Hall–Petch equation rather than coarse-grained powders annealed at high temperatures [5].

4.1.3 XRD analysis of Fe-Ni-Y system

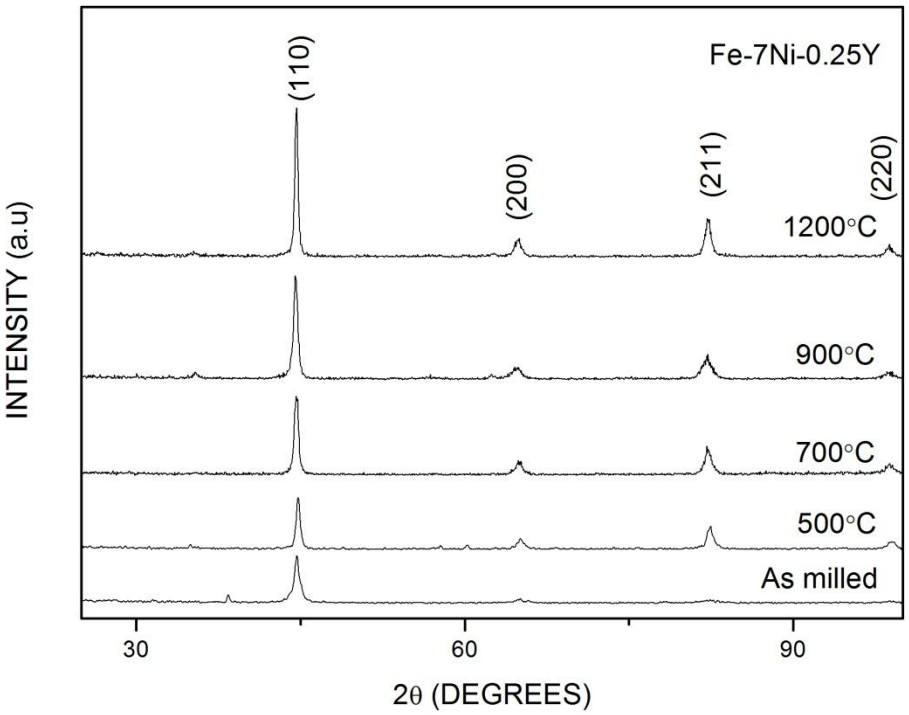

Figure 4.15: XRD pattern of Fe-7 wt.% Ni-0.25 wt.% Y at different temperature

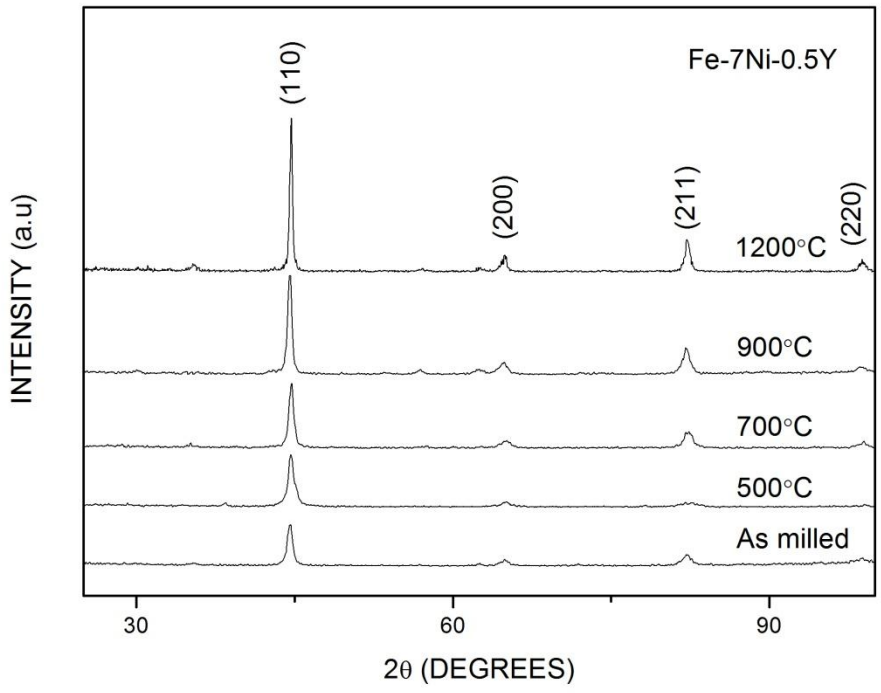

Figure 4.16: XRD pattern of Fe-7 wt.% Ni-0.5 wt.% Y at different temperature

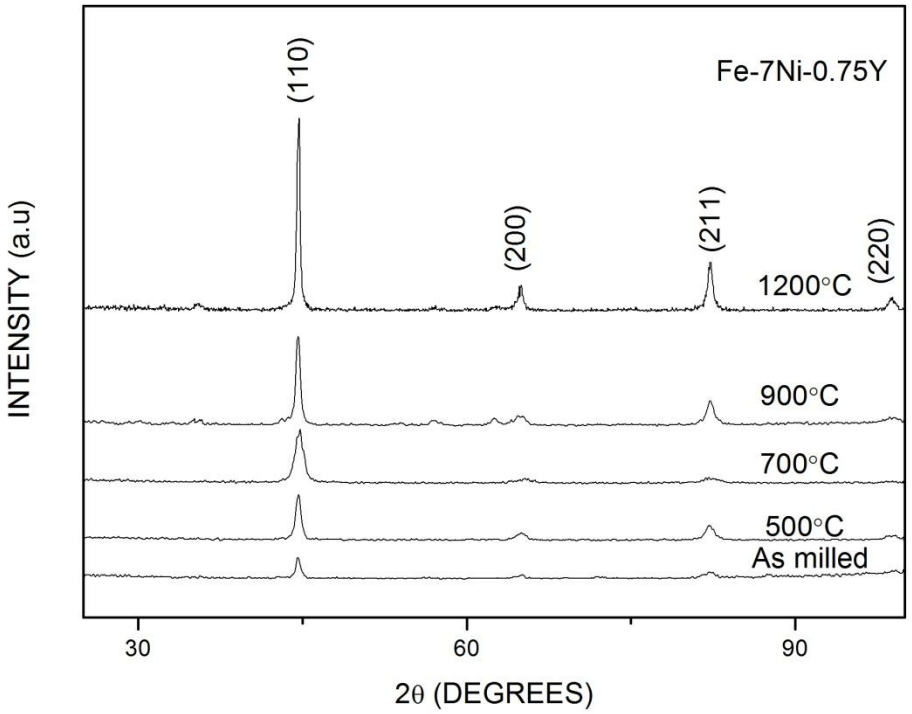

Figure 4.17: XRD pattern of Fe-7 wt.% Ni-0.75 wt.% Y at different temperature

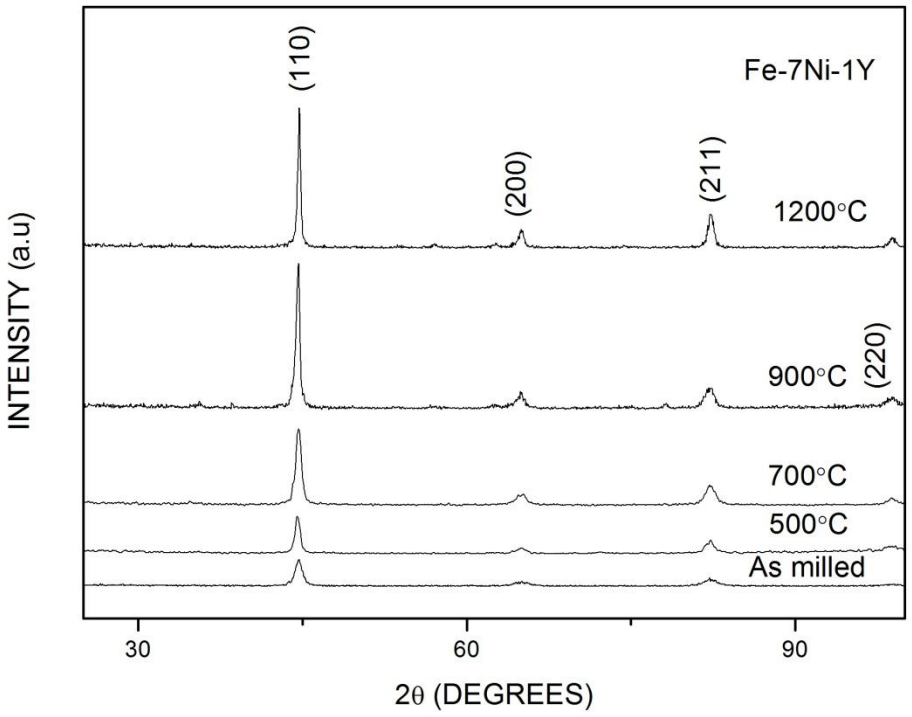

Figure 4.18: XRD pattern of Fe-7 wt.% Ni-1 wt.% Y at different temperature

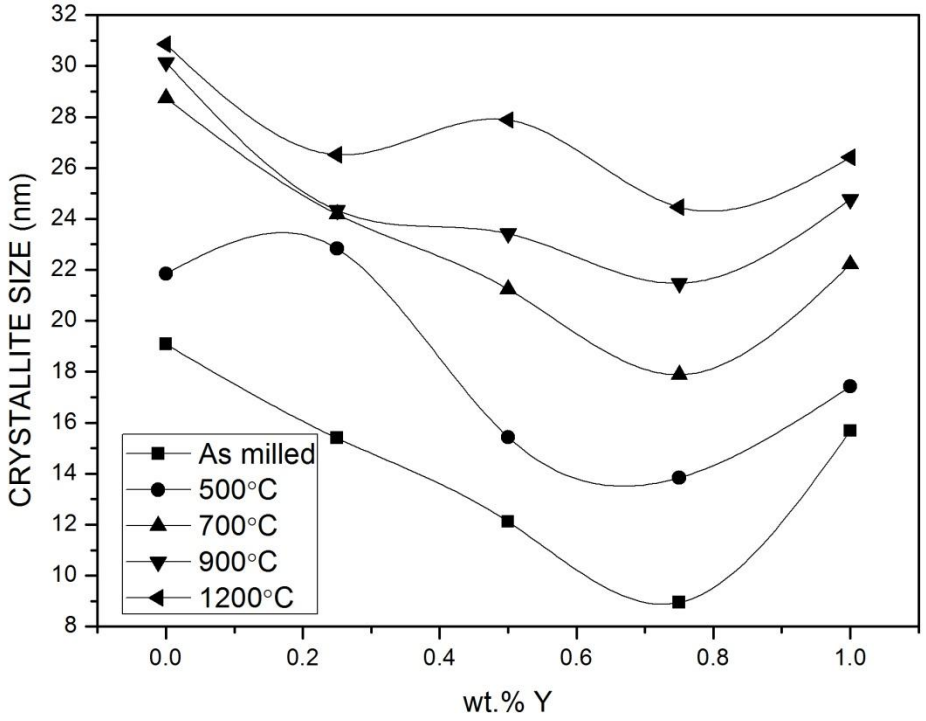

Figure 4.19: variation of crystallite size with different yttrium composition for different temperature

The figure 4.19 shows variation of crystallite size with different yttrium composition for different temperature. From the above figure it is clear that crystallite size decreases prominently with increase in yttrium content up to 0.75 wt. %, but it increases with further addition of yttrium. This happens almost for all annealed samples. A small variation can be seen while annealing at 500℃ and addition of yttrium up to 0.25 wt. %, and for annealing at 1200℃ and while yttrium content increasing from 0.25 wt. % to 0.5 wt. %.

The possible reason for decrease in crystallite size with increase in yttrium content is, the presence of yttrium decrease grain boundary energy and hence provides favourable condition for formation of new and fine grains. Again addition of yttrium more than 1 wt. % leads to adverse effect.

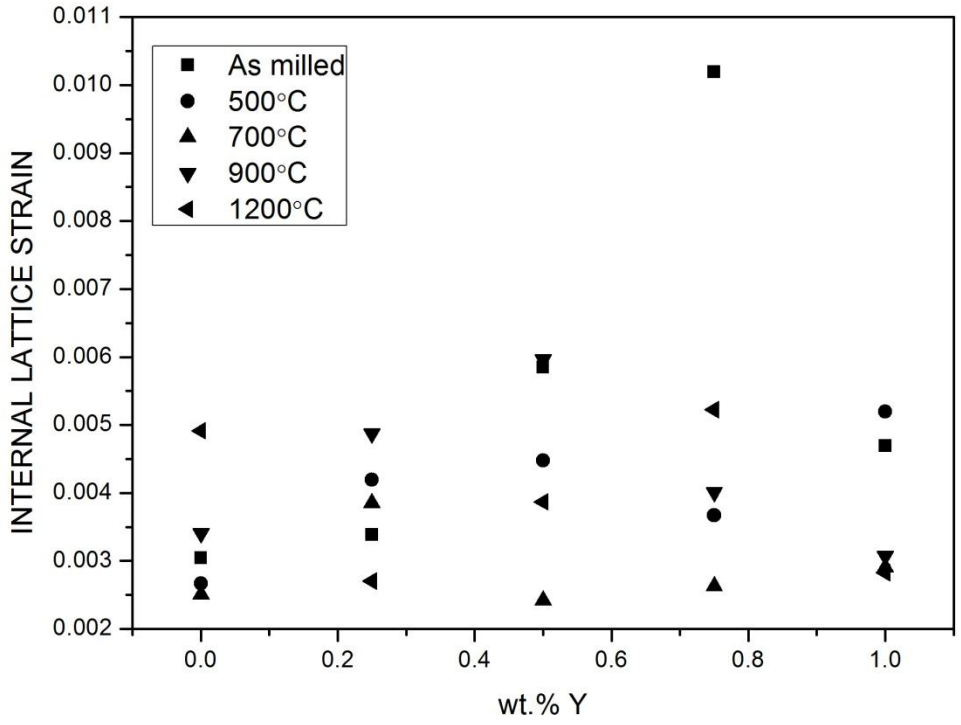

Figure 4.20: variation of Lattice strain with different yttrium composition for different temperature

Figure 4.20 shows variation of Lattice strain with different yttrium composition for different temperature. For as milled samples internal lattice strain increases drastically up to 0.75 wt. %, but further increase leads to decrease in it. This can be seen from XRD graphs. It can be observed that for as milled samples the less is the crystallite size the more is the lattice strain. It is due to dislocations in ball milling of iron based alloys [53].

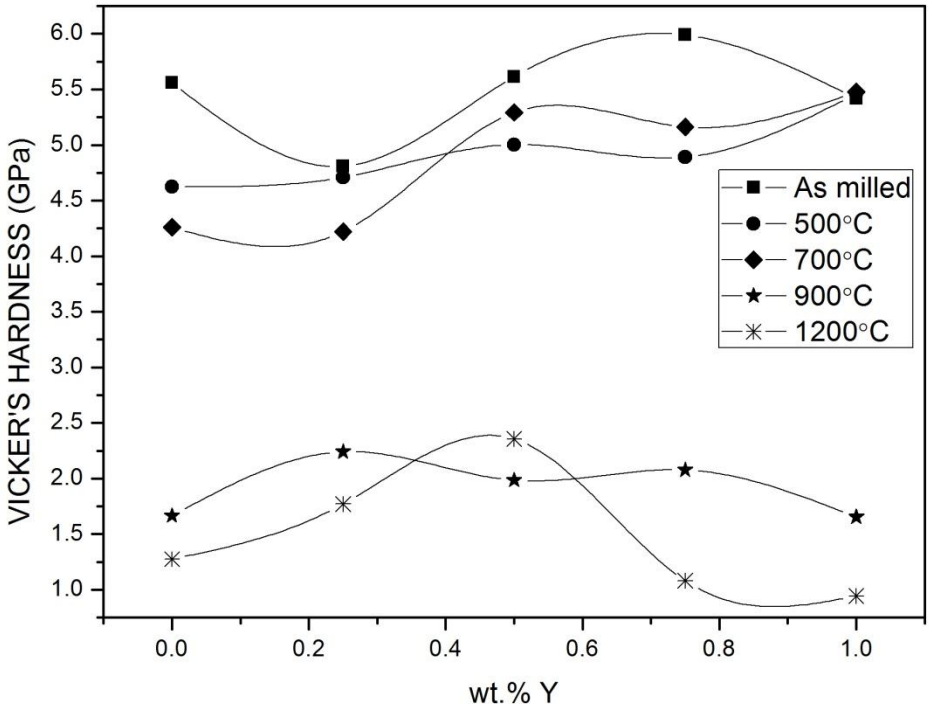

Figure 4.21: variation of Micro hardness with different yttrium composition for different temperature to Fe-Ni

Figure 4.21 shows variation of Micro hardness with different yttrium composition for different temperature to Fe-Ni. It can be seen that Vickers hardness initially decreases, then increases and then reaches to stable condition for as milled samples. Annealing at 500℃ and 700℃ shows increases in hardness over the composition. Micro hardness increases up to 6 GPa for addition of 0.75 wt. % of yttrium to Fe-7Ni.

The hardness can be divided into three categories based on different sources of the strengthening mechanism [56, 57]:

$$H = H_{SS} + H_{Oro} + H_{HP} \quad (14)$$

H is the overall hardness, H_{SS} is the solid-solution strengthening, H_{Oro} is the Orowan mechanism strengthening and H_{HP} is the grain size strengthening. Due to the similar atomic radii Ni in an Fe matrix does not promote significant solid solution hardening. However, solid

solution strengthening can be expected for Y in the as-milled FeNi matrix due to the large atomic misfit.

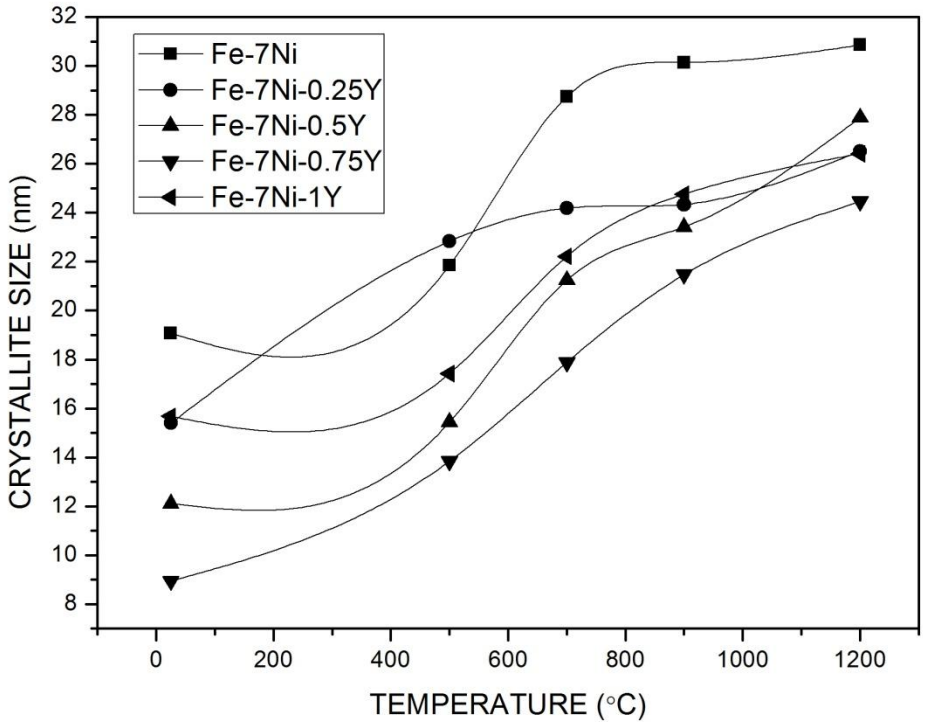

Figure 4.22: variation of crystallite size with different temperature of various compositions

Figure 4.22 shows variation of crystallite size with different temperature of various compositions of Fe-Ni-Y. From the above figure it is clear that crystallite size inecreases with increase in temperature. It becomes stable at higher temperature for Fe-Ni.

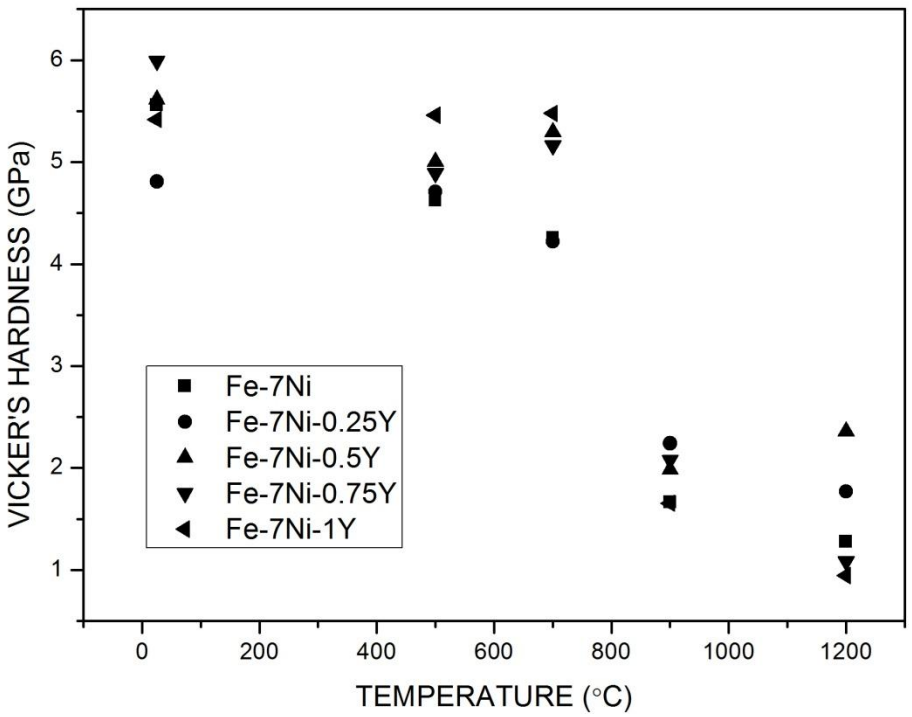

Figure 4.23: variation of Micro hardness with different temperature of various compositions

Figure 4.23 shows variation of Micro hardness with different temperature of various compositions. Annealing at higher temperatures decreases hardness drastically for all the samples. It is due to softening of the material at higher temperature.

The variation in hardness for all the samples at 900℃ is negligible.

4.2 AFM Analysis

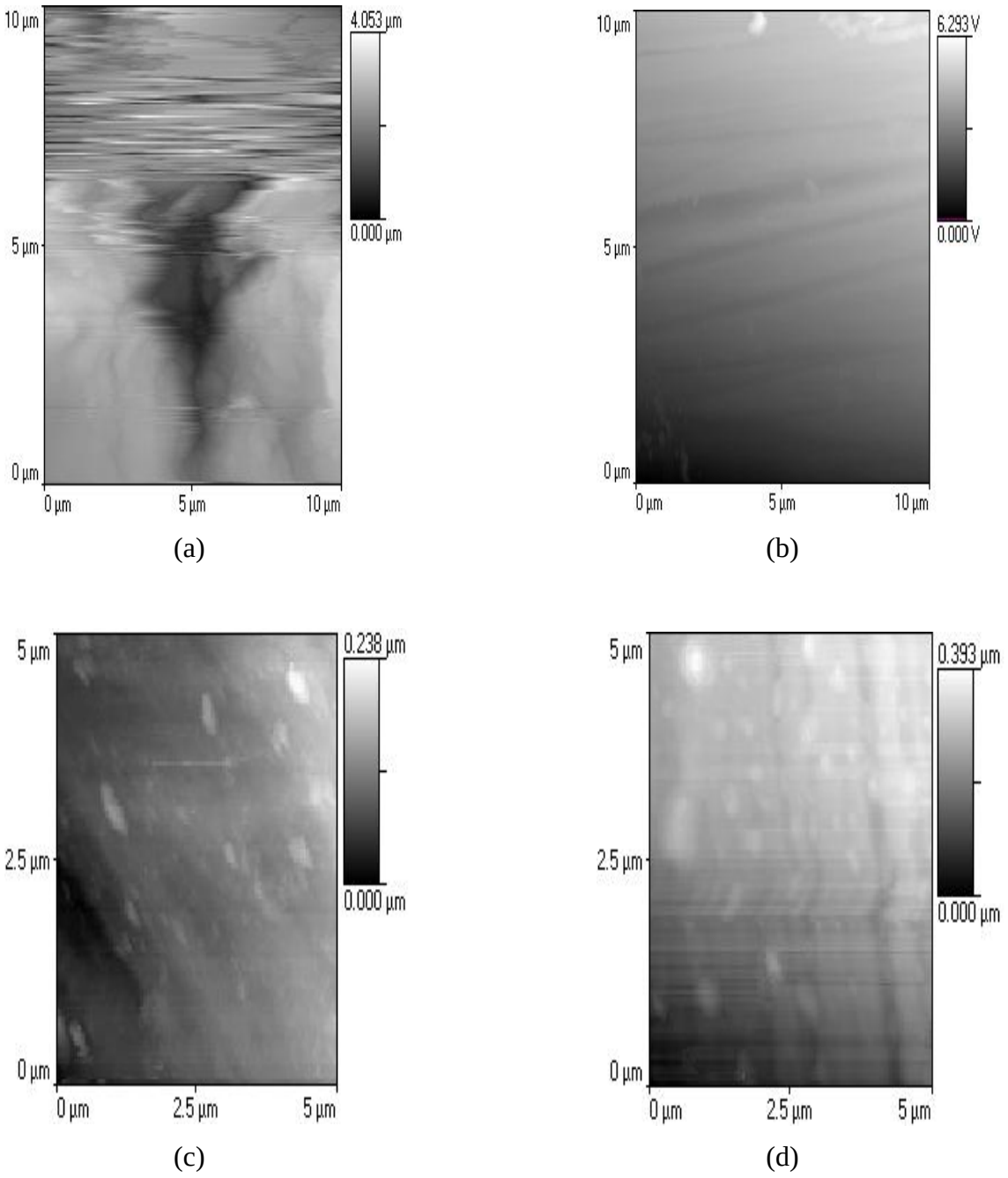

Figure 4.24: AFM data of (a) Fe-0.5Y (at. %) annealed at 700℃ (b) Fe-10Ni (wt. %) annealed at 700℃ (c) Fe-10Ni (wt. %) annealed at 900℃ (d) Fe-7Ni-1Y (wt. %) annealed at 900℃.

Sample	Annealing temperature	Roughness (μm)	Average height (μm)	Grain size (nm)
Fe-0.5Y (at. %)	700℃	0.4343	2.2840	76
Fe-10Ni (wt. %)	700℃	0.7375	4.1928	62
Fe-10Ni (wt. %)	900℃	0.5231	2.1056	58
Fe-7Ni-1Y(wt.%)	900℃	0.0701	0.2351	49

Table 1: Values of the grain size obtained for different samples from AFM

The values of the grain size obtained from AFM best suits the condition of crystallite size obtained by XRD method.

Annealing temperature	Composition									
	Pure Fe	Fe-0.25Y (at. %)	Fe-0.5Y (at. %)	Fe-5Ni (wt. %)	Fe-7Ni (wt. %)	Fe-10Ni (wt. %)	Fe-7Ni-0.25Y (wt. %)	Fe-7Ni-0.5Y (wt. %)	Fe-7Ni-0.75Y (wt. %)	Fe-7Ni-1Y (wt. %)
As milled	7.981	9.184	9.933	6.969	5.559	5.721	4.809	5.614	5.99	5.418
500	6.67	8.414	8.924	6.577	4.626	4.777	4.71	5.004	4.891	5.461
700	4.657	5.664	7.014	6.432	4.259	5.523	4.221	5.293	5.162	5.478
900	3.468	4.336	6.747	2.378	1.666	3.194	2.242	1.985	2.078	1.655
1200	2.654	3.821	5.438	1.67	1.277	2.752	1.771	2.357	1.082	0.945

Table 2: Hardness values (GPa) of samples of different compositions at different annealing temperatures.

CHAPTER 5

CHAPTER 5 Conclusion and Future Scope of Study

- Crystallite size decreases with increase in yttrium content In Fe or Fe-Ni.
- The increase in solute concentration as Y decreases the grain boundary energy, hence the formation of grain boundary requires less energy to be formed. This leads to formation of new and fine grains.
- Addition of yttrium increases hardness from 8 GPa up to 10 GPa for as milled samples. Hardness decreases with increase in temperature, this happens due to increase in crystallite size. Softening occurs due to annealing at higher temperature.
- The possible reason to explain the increase in crystallite size is, the grain boundary energy increases with the increase in Ni content. So formation of new grain boundary to make fine grains is hindered.
- On thermal stability of nanocrystalline Fe, Ni has the less influence and was therefore selected as a control because of its low atomic mismatch and low elastic strain enthalpy.
- Crystallite size inecreases with increase in temperature. It becomes stable at higher temperature for Fe-Ni.
- Dislocations are the primary cause of strain in ball milled iron.
- Micro hardness increases up to 6 GPa for addition of 0.75 wt. % of yttrium to Fe-7Ni, solid solution strengthening is expected for Y in the as-milled Fe-Ni matrix due to the large atomic misfit.

Future Scope of Study

- To study the thermodynamic relation of Fe-Ni-Y system
- To find out magnetic effect of nano structure Fe-Ni-Y system
- To find out corrosion resistance of Fe-Ni-Y system.

CHAPTER 6

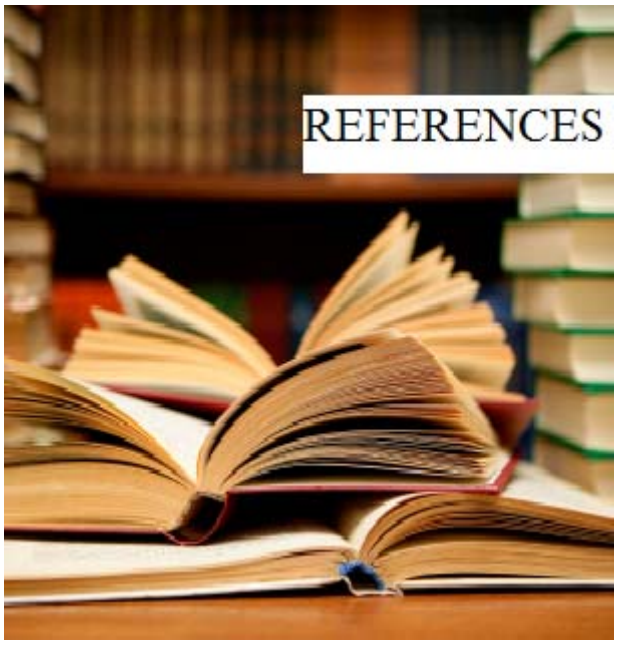

References

1. Daniel mutter, Christine Schieback, Jorg Nedar, Florian Burzale, Kerstin Franzrahe, Annette Gerg and Peter Nielaba, NIC Symposium 2010: Proceedings, 24 - 25 February 2010, Jülich, Germany.
2. M. Aronniemi, J. Sainio, J. Lahtinen, Surface Science, Volume 578, Issues 1–3, 10 March 2005, Pages 108-123
3. K.A. Darling, B.K. VanLeeuwen, J.E. Semones, C.C. Koch, R.O. Scattergood, L.J. Kecskes, S.N. Mathaudhu, Materials Science and Engineering A 528 (2011) 4365–4371
4. LIU Dong-hua, LIU Yong, ZHAO Da-peng, WANG Yan, FANG Jing-hua, WEN Yu-ren, LIU Zu-ming, Transactions Nonferrous Met. Soc. China 20(2010) 831-838
5. H. Kotan, M. Saber, C.C. Koch, R.O. Scattergood, Materials Science and Engineering A 552 (2012) 310– 315
6. D. Cui, J. Jiang, G. Cao, E. Xiao, X. Qu, J. Univ. Sci. Technol. Beijing 15 (2008) 150–154.
7. C. C. Koch, Nanostructured Materials. Vol. 9. pp. 13-22.1997
8. M.A. Meyers, A. Mishra, D.J. Benson, Prog. Mater. Sci. 51 (2006) 427–556.
9. Suryanarayana C. Mechanical alloying and Milling, Progress in Materials Science 46 (2001): pp. 1-184
10. C. C. Koch. (2002). Nanostructured Materials - Processing, Properties, and Applications. William Andrew Publishing.
11. K. Wolski, G. Le Caer, P. Delcroix, R. Fillit, F. Th6venot, J. Le Coze, Materials Sciencea nd EngineeringA 207 (1996) 97-104
12. F. Tehrani, M.H. Abbasi, M.A. Golozar, M. Panjepour, Materials Science and Engineering A 528 (2011) 3961–3966
13. F. Hadefa, A. Otmania, A. Djekounb, J.M. Grenèche, Materials characterization 62 (2011)751 – 759
14. J.Z. Jiang, C. Gente, R. Bormann, Materials Science and Engineering A242 (1998) 268–277
15. T. R. Malow and C. C. Koch, Acta mater. Vol. 45, No. 5, pp. 2177-2186, 1997
16. Atkinson, H. V., Acta metall., 1988, 36, 469-491

17. Bolling, G. F. and Winegard, W. C., Acta metall. 1958,6, 283-287.
18. Grey, E. A. and Higgins, G. T., Acta metall, 1973, 21,309-321.
19. Andersen and O. Grong, Acta metall, mater. Vol. 43, No. 7, pp. 2673-2688, 1995
20. H. Natter, M.-S. Loffler, C.E. Krill and R. Hempelmann, Scripta mater. 44 (2001) 2321–2325
21. J. M. Lifshitz and V. V. Slyozov, J. Phys. Chem. Solids 19, 35 (1961)
22. C. Wagner, Z. Electochem. 65, 581 (1961)
23. J. C. Ion, K. E, Easterling and M. F. Ashby, Acta metall. 32, 1949 (1984).
24. K. Lu, Z.F. Dong, I. Bakonyi, A. Cziraki, Acta Metall. Mater. 45 (1997) 2177
25. Phase transformations in metals and alloys, D.A. Porter, & K.E. Easterling, Chapman & Hall, p140-142.
26. Kunok Chang, Long-Qing Chen, Modelling and simulation in material science and engineering 20 (2012) 055004 (11pp)
27. N. Moelans, B. Blanpain, P. Wollants, Acta Materialia 55 (2007) 2173–2182
28. Azmir Harun, Elizabeth A. Holm, Mike P. Clode, Mark A. Miodownik, Acta Materialia 54 (2006) 3261–3273
29. Zheng Chen, Feng Liu, Xiaoqin Yang, Chengjin Shen, Yu Fan, Journal of Alloys and Compounds 509 (2011) 7109–7115
30. Kris A. Darling, Ryan N. Chan, Patrick Z. Wong, Jonathan E. Semones, Ronald O. Scattergood and Carl C. Koch, Scripta Materialia 59 (2008) 530–533
31. A. Molinari, S. Libardi, M. Leoni, P. Scardi, Acta Materialia 58 (2010) 963–966
32. J. Svejcar, E. Dorazil, P. Pacl, P. Horky, Journal of Magnetism and Magnetic Materials 19 (1980) 45-48
33. Heather A. Murdoch, Christopher A. Schuh, Acta Materialia 61 (2013) 2121–2132
34. G.M. Pharr, W.C. Oliver, MRS Bulletin, 7 (1992), p. 28
35. H.R. Wilde, A. Wehrstedt, Materialprufung, 42 (2001), p. 468
36. C W Nieman, J R Weertman & R W Siegel, scripta Met. et Muter. 23(12),2013 (1989)
37. S K Ganapathi. and D A Rtgney, Scripta Met. Er Mater. 24,1675 (1990)
38. X Y Qin, X J Wu & L D Zhang, Nanostructered Materials, 5 (I), 101 (1995)
39. Yuchui Xiao & R James Kirkpatrick, J. Muter. Res. 10, 10 (1995)
40. Ding, T Tsuzuki, P G McCormick J. Magn. Magn. Mater. 177-181 931 (1998)
41. H. Shokrollahi, Materials and Design 30 (2009) 3374–3387
42. G Li, A Chiba, S Takahashi J. Magn. Magn. Mater. 170 339 (1997)

43. A M Afanas'ev, I P Suzdalev,M Ya Gen, V I Gol'danskii, V P Korneev, E A Manykin Zh. Eksp. Teor. Fiz. **58** 115 (1970)
44. B K Rao, S R de Debiaggi, P Jena Phys. Rev. B **64** 024418 (2001)
45. Yongsheng Liu, Jincang Zhang, Liming Yu, Guangqiang Jia, Chao Jing, Shixun Cao, Journal of Magnetism and Magnetic Materials 285 (2005) 138–144
46. R. Hamzaoui, S. Guessasma, O. ElKedim, E. Gaffet, Materials Science and Engineering B 119 (2005) 164–170
47. Rajeev Gupta, R.K. Singh Raman, Carl C. Koch, Materials Science and Engineering A 494 (2008) 253–256
48. J.L. McCrea, G. Palumbo, G.D. Hibbar an U. Erb, Rev. Adv. Mater. Sci.5(2003) 252-258
49. A. Baron, D. Szewieczek, G. Nawrat, Electrochimica Acta 52 (2007) 5690–5695
50. J. Weissmuller, Nanostruct. Mater. 3 (1993) 261.
51. J. Weissmuller, J. Mater. Res. 9 (1994) 4.
52. A.P. Sutton, R.W. Balluffi, Interfaces in Crystalline Materials, Oxford Press, Clarendon, 1995.
53. F.R. de Boer, R. Boom, W.C.M. Mattens, A.R. Miedema, A.K. Niessen, Cohesion in Metals: Transition Metal Alloys, North-Holland, Amsterdam,1988
54. L. Vitos, A.V. Ruban, H.L. Skriver, J. Kollar, Surf. Sci. 411 (1998) 186
55. A. Revesz, T. Ungar, A. Borbely, J. Lendvai, Nanostruct. Mater. 7 (1993) 779–788.
56. D. Srinivasan, R. Corderman, R. Subramanian, Materials Science and Engineering A 416 (2006) 211.
57. Hasan Kotan, Kris A. Darling, Mostafa Saber, Carl C. Koch, Ronald O. Scattergood, Journal of Alloys and Compounds 551 (2013) 621–629

List of publications

- Debasis Nayak, Suhrit Mula, Analysis and optimization of Material removal rate and Surface Roughness of AISI D2 after EDM process, Processing and fabrication of advanced materials XXI, IIT Guwagati, December 2012, page 931-937